Spatiotemporal Modelling of Soil Organic Carbon Stocks in a Semi-Arid Region Using a Multilayer Perceptron Algorithm

Sébastien Gadal, Mounir Oukhattar, Catherine Keller, Ismaguil Hanadé Houmma

SN Computer Science (2024) 5:561
https://doi.org/10.1007/s42979-024-02872-8

ORIGINAL RESEARCH

Spatiotemporal Modelling of Soil Organic Carbon Stocks in a Semi-Arid Region Using a Multilayer Perceptron Algorithm

Sébastien Gadal[1] · Mounir Oukhattar[1,2] · Catherine Keller[2] · Ismaguil Hanadé Houmma[1,3]

Received: 30 September 2023 / Accepted: 4 April 2024

Abstract

Spatial modelling of soil organic carbon stock (SOCS) and its future dynamics are essential for the sustainable management of terrestrial ecosystems and the planning of carbon sequestration measures. In this study, a spatial modelling approach of the dynamics of the SOCS distribution between 1985 and 2050 and its relationship with land use/land cover (LULC) change in the Béni-Mellal region was accomplished by performing a spatial regression using a multilayer perceptron (MLP) driven by 10 predictors and SOCS data from 40 soil samples. Predictors were extracted from Landsat 5 TM/8 OLI and Sentinel-2 MSI multispectral images and CA-Markov was used for geo-simulations predicting future dynamics. This result shows that the spatial distribution of SOCS and its temporal dynamics in terms of positive and negative variations are strongly linked to spatiotemporal changes in LULC. Over the period 1985–2018, the results showed both progressive variations in the soils of tree crops, unused land and soils in urban areas, slight variations in forest soils and significantly regressive variations in the soils of cropland (− 606 kg.10^6). The future dynamics from 2018 to 2050 suggest a very significant positive evolution of the SOCS in forest soils with a rate of change of 35.6 kg.10^6, while the regressive evolution of the SOCS in cropland should continue at − 73.1 kg.10^6. Furthermore, the spatial autocorrelation results suggest that the spatial distribution of LULC units, topography and vegetation indices are the main factors influencing the quantitative distribution of SOCS in the study area, with correlations ranging from 0.8 to 0.94.

Keywords Soil organic carbon stock · Land use/land cover · Multilayer perceptron · Landsat 5 TM/8 OLI · Sentinel-2 MSI · Semi-arid region

Introduction

Soils are essential to the global carbon cycle and are a precious, non-renewable resource in the context of the human lifespan [1]. They play a crucial role as the basis for agricultural and forestry production. However, soils are under increasing pressure from a variety of sources, leading to conflicts between their different uses [2].

Changes in agricultural production methods, the process of turning over grassland, the increasing conversion of arable or wooded land to urban areas, and the increased extraction of biomass, among other factors, are leading to changes that are potentially harmful to soil quality and the stability of its carbon reserves [3]. As complex systems, soils play an essential role in agricultural and forest ecosystems by orchestrating various natural cycles, including that of greenhouse gases. Because of their agro-environmental functions, soils fulfil a dual role as reservoirs and sinks of organic carbon while at the same time being the source of carbon dioxide (CO_2) emissions into the atmosphere, a major greenhouse gas contributing to the phenomenon of climate change [2, 4, 5].

Soils are the largest terrestrial reservoir of organic carbon, surpassing 2 to 3 the amount present in the atmosphere and 2.5 to 3 times that of the oceans [6]. As a result, they play a key role in the global carbon cycle [3]. Any change, whether positive or negative, in the levels of organic carbon in the soil can lead to emissions or absorptions of atmospheric CO_2 [7]. Changes in land use and development are a major source of man-made greenhouse gas emissions. These soil carbon stocks are highly sensitive to changes in land use and practices, and their state is also influenced by climatic

This article is part of the topical collection "Advances on Geographical Information Systems Theory, Applications and Management" guest edited by Lemonia Ragia, Cédric Grueau and Armanda Rodrigues.

Extended author information available on the last page of the article

Published online: 18 May 2024

conditions. Variations in land use within the agricultural sector (such as grassland conversion) and between agricultural and non-agricultural uses (deforestation, afforestation, urbanisation) have a direct impact on soil carbon stocks and above-ground biomass. Urban expansion at the expense of previously agricultural or natural areas contributes to the overall balance of greenhouse gas emissions [7]. It is therefore crucial to assess the influence of land use and changes in vegetation cover on the quantities of organic carbon stored in the soil.

Various previous studies have examined the impact of land use/land cover (LULC) change on the soil organic carbon stock (SOCS). Some of these studies have concluded that the growth of urbanisation could lead to a decrease in SOCS due to the transformation of soils into impermeable surfaces, which is a consequence of artificialisation [8, 9]. In contrast, other investigations have found higher levels of SOCS in some urban soils than in agricultural areas, grasslands, and forest soils [10, 11].

Previous research focusing on the study area has been relatively limited, concentrating particularly on aspects such as climate change, ecosystem degradation, water-related tensions, and the transformations of LULCs at different times [12–15]. However, no study to date has addressed the spatiotemporal prediction and mapping of soil organic carbon stocks by regression in relation to changes in LULC, associated environmental predictors and topography. The importance of land-use changes over the period 1985–2018 in the study area justifies the need for such investigations.

Spatial modelling of the current and future dynamics of the SOCS is important for many spatial planning and climate change adaptation applications [16]. It has been noted in several studies that SOCS is one of the fundamental characteristics of soil functional health, so its dynamics are a major issue in the current context, where the challenges of climate change are becoming more important. Measurements of soil organic carbon (SOC) content and its spatial modelling can provide reliable and direct indicators of soil quality and fertility, its state of degradation and its potential for SOC sequestration [17]. Very often, SOCS samples from point locations and environmental, topographical and pedoclimatic predictors are used in models of spatial predictions of SOCS distribution [18]. Proximal detection methods (visible, infrared, and mid-infrared spectroscopy) are the most widely used techniques for estimating SOC content in soil samples [19, 20]. However, although these methods are accurate, they are limited when we are interested in spatially continuous assessment of the SOCS concentration. For this reason, geostatistical approaches and deep and machine learning models have been introduced for the purposes of spatial modelling of SOC content [18, 21]. Geostatistical methods such as inverse distance weighting (IDW) and ordinary kriging (OK) have been used in several studies to overcome the limitations of conventional approaches, which are considered too simplistic and do not provide detailed spatially continuous information on the distribution of the SOC stock [22–24]. Nevertheless, although these spatial interpolation methods are an alternative to conventional methods of estimating the SOCS, particularly in unmeasured areas, they also have several limitations. The lack of precision in the estimates is one of the limitations of spatial interpolation methods, linked to the fact that some techniques assume intrinsic stationarity, which may not be systematically appropriate in practice [22, 23]. In addition, it is often pointed out that many kriging techniques are only effective if the target variable is normally distributed [24]. To overcome the limitations of geostatistical methods, spatial modelling of soil organic carbon stocks has gained popularity in recent years [24–28]. These methods have the advantage that they make no assumptions about the normality of the spatial and/or temporal distribution of the variable of interest or the geo-environmental predictors. However, geostatistical methods can be used in conjunction with machine learning and/or deep learning methods to model the spatial distribution of SOCSs more accurately [24, 29].

Similarly, remote sensing and spatial modelling techniques based on deep learning and machine learning have been widely adopted in recent decades. They are used to quantify the spatiotemporal distribution of environmental variables such as changes in land cover and land use and organic carbon stocks in the soil [7, 30–33]. Numerous studies have used these remote sensing and spatial modelling methods to specifically assess changes in land use and their potential impact on soil organic carbon stocks [7, 34, 35]. This research has highlighted the crucial importance of remote sensing from space in creating models that trace past and present trends, enabling future forecasts to be made [36, 37]. Certain artificial intelligence (AI) models have been used to anticipate future changes in land use and soil organic carbon reserves and to assess their potential environmental impact. References such as [38] and [39] have summarised the models most used to assess land use dynamics.

Markov chain analysis and the multilayer perceptron (MLP) are artificial intelligence approaches that can be easily used to predict the spatial characteristics of LULCs, and SOCSs based on current situations [40–43]. In addition, because these approaches offer the ability to examine historical trends, we adopted them to estimate and predict the rate of change in LULC categories and the spatial distribution of SOCS within our study area for the period from 1985 to 2050. Soil analyses were carried out to characterise the physical parameters of the soil, including texture, density, and organic carbon content, while remote sensing and spatial modelling were used to assess changes in LULCs and the spatial distribution of SOCS.

In the United States, a study conducted by [44] compared variations in soil organic carbon stocks in six different cities (Atlanta, Baltimore, Boston, Chicago, Oakland, and Syracuse), revealing that urban soils have significant potential for sequestering substantial quantities of atmospheric carbon dioxide (CO_2). This investigation showed that urban green spaces had higher soil organic carbon reserves than native prairies, agricultural areas, or forests in the state of Colorado in the United States [10]. The work of [45] showed that the surface carbon reserves in the soils of the urban forests of Seattle in Washington were comparable to those present in the Amazon rainforest. In addition, [46] undertook an assessment of the above-ground net primary productivity of urban lawns, concluding that this productivity was four to five times higher than that of the surrounding farmland and grassland. In addition, research by [47] found that urban infrastructure such as roads, waterways and grass-covered railways accounted for approximately 15% of the total SOCS in an urban area. It should also be noted that soils underlying impermeable surfaces in urban areas are an often-overlooked source of SOC [11, 48].

In 2008, Morocco adopted the Green Morocco Plan (GMP) as a development strategy for the agricultural and rural sectors. The aim of this initiative is to position Moroccan agriculture as a driver of economic and social growth while seeking to resolve several constraints hindering the sustainability of this development [49]. First and foremost, this strategy aims to reduce spatial disparities, which remain significant and could worsen because of unequal access to the resources needed for agricultural development. Spatial planning and agricultural territorialisation are essential to meeting this challenge. This means adapting development approaches to each region, capitalising on the strengths of different rural areas and mitigating their vulnerabilities. These vulnerabilities include the fragility of agricultural land, which a policy of sustainable management and preservation can help overcome. Second, the GMP also seeks to resolve the complex issue of land tenure status in Morocco, which is at the root of various forms of deterioration, particularly for state-owned land and land with community status. The land tenure system reform aims to increase local players' responsibility in the preservation and rational management of natural resources [49].

The aim of this study is to predict SOC stocks by spatial modelling using the MLP deep learning model, considering environmental variables, transformations, and spectral bands. In addition, it aims to assess the influence of factors such as LULC in different classes, such as tree crops, cropland, urban areas, unused land, and forest areas. This approach is crucial for monitoring the rapid, unregulated changes caused by urbanisation, which is often uncontrolled and poses a threat to the SOCS. Rapid urbanisation, characterised by the growth of towns and infrastructures, tends to develop at the expense of natural and agricultural areas, generally leading to land and soil degradation. This degradation has harmful consequences for the environment, leading to major problems such as erosion, landslides, loss of biodiversity, an increase in the concentration of CO_2 in the atmosphere, desertification, and groundwater pollution [50]. It is therefore essential to carry out spatial modelling studies of SOCS using geo-environmental predictors to promote environmental sustainability. Spatial and temporal analysis of trends in LULC and SOCS and study of the relationships between the factors influencing these variations would enable better management of land and soil use. This approach would also make it easier to make informed decisions about urban development and the protection of environmental resources, particularly regarding soil carbon sequestration. The main stages of this study are: (1) Mapping LULC in 1984, 2000, and 2018 using Landsat 5 TM (Thematic Mapper), Landsat 8 OLI (Operational Land Imager), and Sentinel-2 MSI (Multispectral Instrument) images to understand the changes in LULC over time. (2) The geo-simulation of LULC evolution in the Béni-Mellal region to 2030 and 2050 by Markov chain probabilistic simulation based on LULC mapping (1985-2018). (3) Soil sampling in the different LULC classes to measure SOC content, SOC stock and soil texture. (4) Prediction of the spatiotemporal soil organic carbon stock evolution (1985-2050) by modelling using a deep learning approach, environmental covariates, and spectral transformations. (5) Spatial correlations between soil organic carbon stocks, environmental covariates, spectral transformations and spectral bands from the Landsat 8 OLI and Sentinel-2 MSI satellites for 2018. These spatial correlations make it possible to identify and compare the important factors affecting soil organic carbon stocks, as mapped from the data acquired by these two satellites. (6) Evaluate and compare the overall accuracy of the LULC and SOCS maps mapped for 2018 using data from the Landsat 8 OLI satellite with a spatial resolution of 30 m and the Sentinel-2 MSI satellite with a spatial resolution of 10 m.

This study is an extension of the conference proceedings GISTAM 2023: 9th International Conference on Geographical Information Systems Theory, Applications and Management [51], which initiated an analysis of spatial autocorrelations between land use change, organic carbon stocks, environmental covariates, and spectral transformations. In contrast, this study focuses specifically on a spatiotemporal analysis of the current (1985–2018) and future (2018–2050) dynamics of the spatial distribution of SOCS in relation to changes in LULC. To refine the study, statistical analyses were carried out to validate the results, additional mapping was carried out, and the effect of using Sentinel-2 MSI high spatial resolution (10 m) multispectral images from 2018 was compared with the LULC classification and SOCS spatial modelling using Landsat 8 OLI data of 30 m spatial

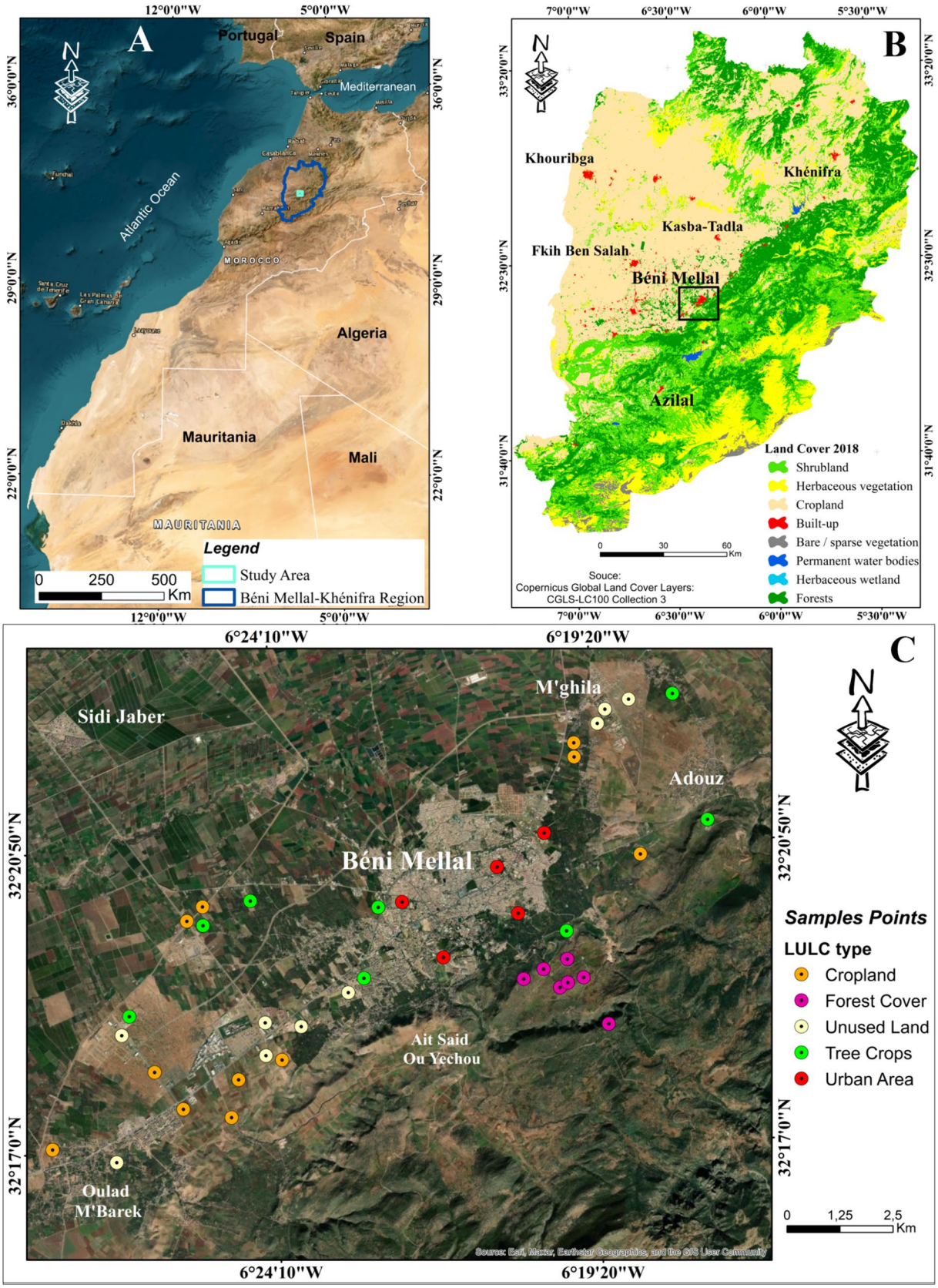
A
Portugal
Spain
Mediterranean
Atlantic Ocean
MOROCCO
Algeria
Mauritania
Mali
MAURITANIA
Legend
Study Area
Béni Mellal-Khénifra Region
0 250 500 Km
12°0'0"W
5°0'0"W
36°0'0"N
29°0'0"N
22°0'0"N
B
Khouribga
Khénifra
Kasba-Tadla
Fkih Ben Salah
Béni Mellal
Azilal
Land Cover 2018
Shrubland
Herbaceous vegetation
Cropland
Built-up
Bare / sparse vegetation
Permanent water bodies
Herbaceous wetland
Forests
0 30 60 Km
Souce:
Copernicus Global Land Cover Layers:
CGLS-LC100 Collection 3
7°0'0"W
6°30'0"W
6°0'0"W
5°30'0"W
33°20'0"N
32°30'0"N
31°40'0"N
C
Sidi Jaber
M'ghila
Adouz
Béni Mellal
Ait Said
Ou Yechou
Oulad
M'Barek
Samples Points
LULC type
Cropland
Forest Cover
Unused Land
Tree Crops
Urban Area
0 1,25 2,5 Km
6°24'10"W
6°19'20"W
32°20'50"N
32°17'0"N

◂**Fig. 1** **A** Geographical position of the study area in Morocco, **B** geographical position of the study area in Béni Mellal-Khénifra region (source: land cover map 2018 of the Béni Mellal-khénifra area: Copernicus Global Land Cover (https://lcviewer.vito.be/2018). The map was downloaded from the Google Earth Engine platform with a spatial resolution of 100 metres via the following link: https://developers.google.com/earth-engine/datasets/catalog/COPERNICUS_Landcover_100m_Proba-V-C3_Global#description), and **C** spatial distribution of sampling sites for each type of LULC in the study area

resolution from the same year. To this end, the effect of improving the high spatial resolution on the performance of the image classification algorithm spectral angle mapper (SAM) and the spatial predictions of the SOCS (MLP) were evaluated and analysed.

Materials and Methods

Study Area

The study area is in the Béni Mellal-Khénifra region, province of Béni-Mellal, Morocco (32° 15′ 35″–32° 23′ 22″ N; 6° 27′ 54″–6° 16′ 44″ W). It covers an area of 252.5 km^2 with a perimeter of 63.9 km at the foot of the Middle Atlas Mountains (see Fig. 1). The region overlooks the irrigated agricultural plain of Tadla, renowned for its production of citrus fruits, olives, figs, sugar beet and cereals.

The altitude in the region varies from 439 m in the northwest to 1709 m (Jabal Tassemit) in the southeast. Administratively, it encompasses the communes of Sidi Jaber, Ouled M'barek, Adouz and Béni-Mellal. The population rose from 192 676 in 2014 to 209 563 in 2020. This region benefits from significant water resources from the Atlas Mountains and has vast tracts of fertile land [14, 52], making it an area of high agricultural production. Agriculture and livestock farming are the main economic activity and income sectors, with olives and citrus fruits as the region's main tree crops.

The climate in the Béni-Mellal region is typically semi-arid, with average annual rainfall ranging from approximately 350 to 650 mm, of which almost 87% falls between October and March. Rainfall is less abundant in summer than in winter. The average annual temperature is 14.17 °C, with an average minimum temperature of 1.1 °C observed in January and an average maximum temperature of 30°C in July and August. The average annual rainfall varies between 350 and 650 mm, of which approximately 87% falls between October and March.

Soils in the study area play a significant role in various categories, including the following types: isohumic, subtropical brown or chestnut soils are predominant [53]. They cover the vast majority of the Tadla plain, occupying almost 83% of the irrigated area. These soils have a clayey or balanced texture and offer conditions that are conducive to the development of irrigated agriculture. On the other hand, shallow, calcimagnesic brown soils, which are highly calcareous and stony but have a balanced texture, are located along the wadis. They make up approximately 11% of the soil composition in the Béni-Mellal region [53].

To validate the LULC change maps, the validation points (the 40 sampling sites) shown in Fig. 1 are mainly used. At the same time, each validation point was associated with soil sampling, enabling the determination of soil organic carbon content, soil organic carbon stock and soil texture for the distinct types of LULC.

Data and Methods

Data and Preprocessing

In this study, the LULC maps for the years 1985 and 2000 were generated using images from the Landsat 5 TM satellite. Similarly, the LULC maps for 2018 were generated using images from two different sensors: the image from the Landsat 8 OLI satellite and the image from the Sentinel-2 MSI satellite (Table 1).

The Landsat 5 TM/8 OLI images supplied have a spatial resolution of 30 metres, except for the thermal infrared band for Landsat 5 TM images, which has a resolution of 120 m, and the panchromatic band for Landsat 8 OLI images, which has a resolution of 15 m. The Sentinel-2 MSI satellite image encompasses a total of thirteen spectral bands, ten of which cover the visible to short-wave infrared range. Of these, four bands have a spatial resolution of 10 metres (blue, green, red and near infrared), while six bands offer a resolution of 20 metres, covering the red edges of vegetation and two short-wave infrared bands.

The spatial data were all referenced to the same coordinate system: "WGS 1984 UTM Zone 29 N". The satellite images used in this study were captured during the dry summer period, specifically on 4 July 1985, 13 July 2000, 23 June 2018, and 29 June 2018 (Table 1). This selection aims to minimise errors induced by seasonal variations and the specific effects of the seasons on agricultural crops in the Béni-Mellal region. The ASTER GDEM digital elevation model (DEM) was acquired on 23 September 2014, with a spatial accuracy of 30 metres.

All the images used in this study, which were taken at different time periods (Landsat 5 TM/8 OLI and Sentinel-2 MSI), were subject to radiometric calibration (RC) and corrections to eliminate dark artefacts "dark subtraction (DS)". For the 2018 Sentinel-2 MSI image, the red-green-blue (RGB) colour bands and the near-infrared (NIR) band were superimposed and then cropped to cover the area of interest. The Gram−Schmidt Pan Sharpening (GSPS) algorithm was used to adjust this image to a resolution of 10 metres. The 2018 Landsat 8 OLI image to calibrated at a spatial

Table 1 Satellite data characteristics

Data	Landsat 5 TM		Landsat 8 OLI	Sentinel-2 MSI	ASTER GDEM
Date of images	1985	2000	2018	2018	2014
Acquisition date	4 July 1985	13 July 2000	29 June 2018	23 June 2018	23 September 2014
Projection	WGS_1984_UTM_Zone_29 N				
Spatial resolution	30–120 m		15–30 m	10–60 m	30 m
Source	earthexplorer.usgs.gov			https://scihub.copernicus.eu/	earthexplorer.usgs.gov

resolution of 15 metres. This decision was made to simplify the comparison of the accuracy of LULC classifications and SOCS regression results by using two clearly distinct resolutions: 10 metres (Sentinel-2 MSI) and 30 metres (Landsat 8 OLI), thus offering a significant margin. This approach is preferable to using resolutions of 10 metres (Sentinel-2 MSI) and 15 metres (Landsat 8 OLI), which offer little significant difference.

All raster images of the study area were cut according to a rectangular polygon created to cover the specific study area. Each raster image was then subjected to classification to generate the LULC maps. Field data and the Google Earth platform were used to identify five LULC categories: urban areas, forest cover, unused land, cultivated land and tree crops. The spectral angle mapper (SAM) supervised classification method was used to perform classification, enabling the derivation of all predefined LULC categories (Fig. 2).

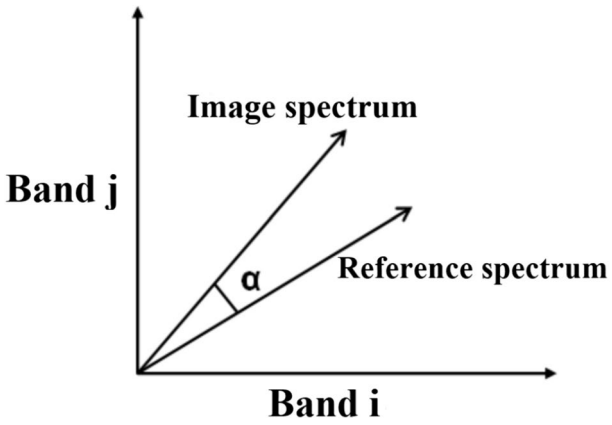

Fig. 2 Principle of SAM classification (reference: [56])

Spectral Angle Mapper (SAM)

The spectral angle mapper (SAM) method is a supervised classification approach based on measuring the angular similarity between the individual spectrum of each pixel in an image and reference spectra known as endmembers [54]. These endmembers can be obtained directly in the field using a spectroradiometer or extracted from the image itself. The assignment of a pixel to a specific class is determined by the value of the angle "α", which quantifies the similarity or divergence between the reference spectrum vector and the corresponding spectrum of the pixel in the image [55]. As a result, the pixel is assigned to the spectral class with the greatest similarity; in other words, when the angle "α" is small, this reflects a strong match between the evaluated spectrum of the pixel and the reference spectrum (Fig. 2) [56].

In our context, the prototype spectral signatures used to perform the SAM method were derived from the image itself. These signatures represent five distinct land cover classes (i.e. tree crops, cropland, unused land, urban areas, and forest cover). In this study, following a visual evaluation and comparison of LULC classification results from six supervised classification algorithms (namely, support vector machine, spectral angle mapper, parallelepiped, minimum distance, maximum likelihood and Mahalanobis distance), the SAM algorithm was found to have the most satisfactory supervised classification performance. Consequently, the SAM algorithm was used to classify the five main land cover classes in our study area.

Collecting and Analysing Soil Samples to Measure SOCS

Soil sampling sites were identified using their GPS coordinates and selected according to LULC categories using the Google Earth platform and the LULC map generated in 2018 from Landsat 8 OLI data (see Fig. 5C). A total of 40 locations were selected for sampling, comprising 8 points in the woodland category, 11 in the cropland category, 9 in the undeveloped land category, 5 in urban areas and 7 in the forest cover category. These samples were taken on 26 April 2019 and 03 May 2019 at a depth of 0 to 15 cm due to limitations at the laboratory preventing sampling across the entire soil profile. The geographical coordinates of the sites sampled were recorded in the field using a global positioning system (GPS).

Each soil sampling site was provided with 3 samples taken approximately 10 m apart. These intact soil samples were obtained using a metal cylinder measuring 15 cm in height and 9 cm in diameter, which was then used

to calculate the apparent density of the soil based on the volume of the cylinder ($V_{cylinder} = 396.3\ cm^3$). All the samples were dried in an oven in the soil analysis laboratory at the Faculty of Science and Technology in Béni-Mellal at a temperature of 40°C for a period of 48 hours until their weight stabilised.

The dried soil was then sieved to a particle size of 2 mm to separate coarse fragments larger than 2 mm. The volume of coarse fragments (>2mm) thus obtained was measured using a graduated cylinder, enabling the soil's bulk density (BD) to be calculated (Eq. (1) proposed by [57] and [58]). The fraction of particles smaller than 2 mm was recovered and ground into a fine, homogeneous powder using an agate mortar. This fraction will then be analysed to determine the organic carbon content. To measure the texture of the soil, we used the fraction of particles smaller than 2 mm.

$$\mathrm{BD}\left[\frac{\mathrm{g}}{\mathrm{cm}^3}\right] = \frac{\left(\text{total mass of dry soil}\left[\mathrm{g}\right] - \text{mass of coarse fragments}(>2\mathrm{mm})\left[\mathrm{g}\right]\right)}{\left(\text{total volume of dry soil}\left[\mathrm{cm}^3\right] - \text{volume of coarse fragments}(>2\mathrm{mm})\left[\mathrm{cm}^3\right]\right)}. \quad (1)$$

Soil organic carbon (SOC) content was assessed using soil organic matter (SOM), determined using the incineration method, also known as the loss on ignition method. Loss on ignition is a direct measure of the amount of organic matter present in the soil. The samples were placed in a muffle furnace preheated to 540 °C and kept there for a period of 4 hours. The weight reduction observed after calcination was used to estimate the soil organic matter (SOM) content. The SOM content was determined using equation (2).

$$\mathrm{SOC}[\%] = \frac{\mathrm{SOM}[\%]}{1.724}. \quad (2)$$

The coefficient 1.724 (calculated as 100/58) is used as a conversion coefficient, although its value can fluctuate depending on soil characteristics. Nevertheless, for most applications, a reasonable estimate of soil organic matter can be obtained using the coefficient 1.724 [58]. It is important to note that this conversion coefficient assumes that organic matter contains 58% organic carbon. However, this proportion can vary according to the type of organic matter, soil type and soil depth. Higher conversion coefficients, up to 2.5, are possible, particularly for subsoils [59].

In this context, it should be noted that SOC refers to soil organic carbon content as a percentage, while SOM refers to soil organic matter as a percentage. After measuring the soil organic carbon content and determining the bulk density of the soil and the volume of coarse fragments (> 2 mm) in the samples, we calculated the soil organic carbon stock using the following formula (3) proposed by [60, 61] and [62]:

$$\mathrm{SOC}_{\mathrm{Stock}}\left[\frac{\mathrm{kg}}{\mathrm{m}^2}\right] = SOC_{Content} \times \mathrm{BD} \times \mathrm{Depth} \times \frac{\left(1 - \mathrm{Coarse}_{volumefraction}\right)}{10}, \quad (3)$$

where Depth = 15 cm, $\mathrm{SOC}_{Content}$ is the organic carbon content expressed in (%), BD is the bulk density expressed in (g/cm^3), 0.1 is a conversion factor to convert Mg/ha to kg/m^2 and $\mathrm{Coarse}_{volumefraction}$ is the volume fraction of coarse fragments (without unit) [63].

The total stocks of SOC for each LULC type expressed in ($kg.10^6$) in the study area were calculated according to the following equation (4):

$$\text{Total SOCS}_j = \mathrm{SOCS}_{average,j} \times \mathrm{Area}_j, \quad (4)$$

where j represents each LULC type (i.e. tree crops, cropland, unused land, urban areas, and forest cover). *Total SOCSj* is the total soil organic carbon stock for LULC type j. $SOCS_{average,j}$ is the average soil organic carbon stock for LULC type j. $Area_j$ is the surface area in km^2 for LULC type j. This means that for each LULC type, the total soil organic carbon stock is calculated by multiplying the average soil organic carbon stock for that type by the total area of that LULC type.

Granulometric analysis was used to measure soil texture. This method involves separating the mineral fraction of the soil into different categories according to the size of the mineral particles, with a lower limit of 2 mm. The relative proportions of these categories (sand, silt, clay) are then determined as a percentage of the total mass of the mineral fraction of the soil. The textural classifications were established in accordance with the classification scheme developed by the United States Department of Agriculture (USDA) [64].

Prediction of Future LULC and SOCS Dynamics

The Markov cellular automaton model (CA-Markov) was used to geo-simulate the evolution of LULC and SOCS up to 2030 and 2050. CA-Markov is a probabilistic model of temporal/environmental/simulation change based on the LULC maps generated by the SAM classifier between 1985 and 2018 and on the SOCS, maps predicted by the MLP model over the same period.

Classified LULC maps and SOCS predictions for 1985, 2000 and 2018 were used to study dynamic changes between 1985 and 2018, generating intermediate maps of potential

transitions and a transition probability matrix from 1985 to 2018, from 2018 to 2030 and from 2018 to 2050. In this way, the transition probabilities and suitability zones were created by running the probabilistic Markov matrix before carrying out the geo-simulation with CA-Markov [65, 66].

Spatial Distribution of Soil Organic Carbon Stock Using MLP

Satellite images from Landsat 5 TM in 1985 and 2000, as well as Landsat 8 OLI (L8) and Sentinel-2 MSI (S2) in 2018, were used to map the LULC, calculate vegetation indices and perform spectral transformations. After preprocessing the satellite images (radiometric and atmospheric corrections for the Landsat 5 TM/8 OLI images and resampling for the Sentinel-2 MSI image - part 2.2.1), a total of four vegetation indices were calculated, namely, the normalised difference vegetation index (NDVI), the soil adjusted vegetation index (SAVI), the ratio vegetation index (RVI) and the enhanced vegetation index (EVI). In addition, principal component analyses (PCA) and minimum noise fraction (MNF) of spectral bands were used. A digital elevation model (DEM) was also included as a topographic variable in the study area (Table 2).

In this study, a multilayer perceptron (MLP) deep learning model was fitted using data from 1985, 2000 and 2018 from Landsat 5 TM/8 OLI and Sentinel-2 MSI imagery. The MLP model was applied to estimate soil organic carbon stocks by regression using remote sensing data collected for the periods 1985, 2000 and 2018, as well as field data collected in 2019.

The MLP, which is the most important and most used structure in artificial neural networks (ANNs), is a non-parametric estimator used for the regression of SOC stocks [35]. This method is based on highly interconnected neurons organised into layers comprising an input layer, one or more hidden layers and an output layer. Data are fed into the network via the input layer and then passed to the hidden layers, where they are processed before being routed to the output layer. The MLP's capacity comes from the nonlinear processing carried out in the hidden layers [67].

To estimate SOCS to a depth of 15 cm, the MLP model integrates environmental covariates, spectral transformations, and colour composition images, as well as in situ SOCS data measured at the 40 sites sampled and analysed. Environmental covariates such as NDVI, SAVI, EVI, RVI, LULC, DEM, MNF and PCA spectral transformations, as well as RGB (spectral bands in the red, green, and blue) and NIRGB (spectral bands in the near-infrared, red, green, and blue) colour composition images, were included in the MLP model as images representing independent variables. The SOCS measurements were integrated as a dependent image after their spatial interpolation using the kriging method (Fig. 3). After SOCS estimation for 1985, 2000 and 2018, we used the CA-Markov machine learning model to project and predict SOCS maps for 2030 and 2050 (Fig. 4). These SOCS projections for future years are crucial for understanding the potential evolution of soil carbon sequestration in our study area. They can also be used to inform natural resource planning and management by highlighting areas that could experience significant changes in soil organic carbon stock over time.

Overall Accuracy of LULC and SOCS Maps of 2018

The 2018 LULC maps from Landsat-8 OLI and Sentinel-2 MSI were validated using 2018 "natural" RGB colour composition images from the worldview-3 satellite with a resolution of 30 cm by visualisation on the Google Earth platform. To do this, 20 ground control points in each LULC type (tree crops, cropland, unused land, urban

Table 2 Characteristics and categorisation of the SOCS predictor variables

Variables	Description	Spatial resolution	Source
DEM	Provide a three-dimensional representation of the terrain and enable analysis of topographical features.	30 metres	ASTER GDEM
MNF	Reduce noise and improve the signal-to-noise ratio of an image.	30 meters and 10 meters	Landsat 5 TM/8 OLI and Sentinel-2 MSI
PCA	Reduce the dimensionality of the data and extract the most important features.		
NDVI EVI SAVI RVI	Measure the amount of vegetation in our study area and analyse the vegetation cover, which can affect soil organic carbon stocks.		
RGB NIRGB	Analyse the reflectance of different wavelengths of light.		
LULC	Provide information about the type of land cover and land management practices that can affect soil organic carbon stocks.		

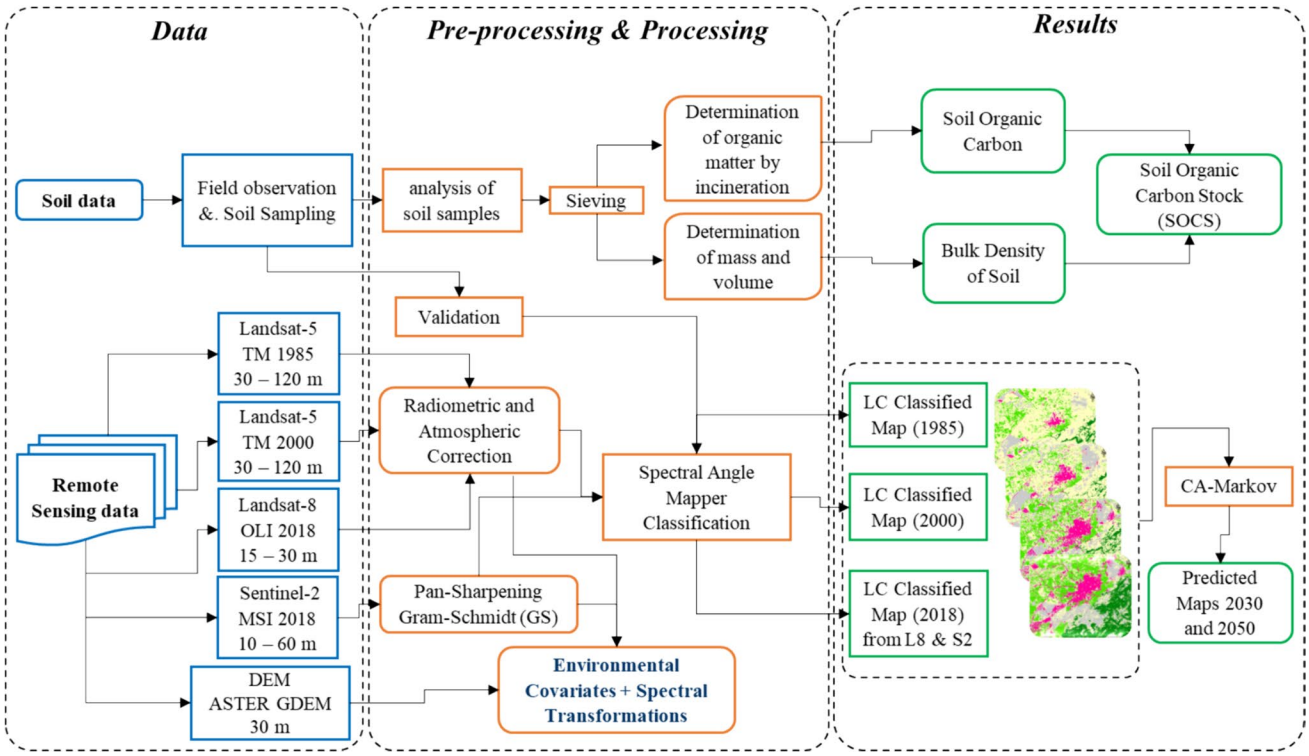

Fig. 3 Flowchart of the methodology used in the study area

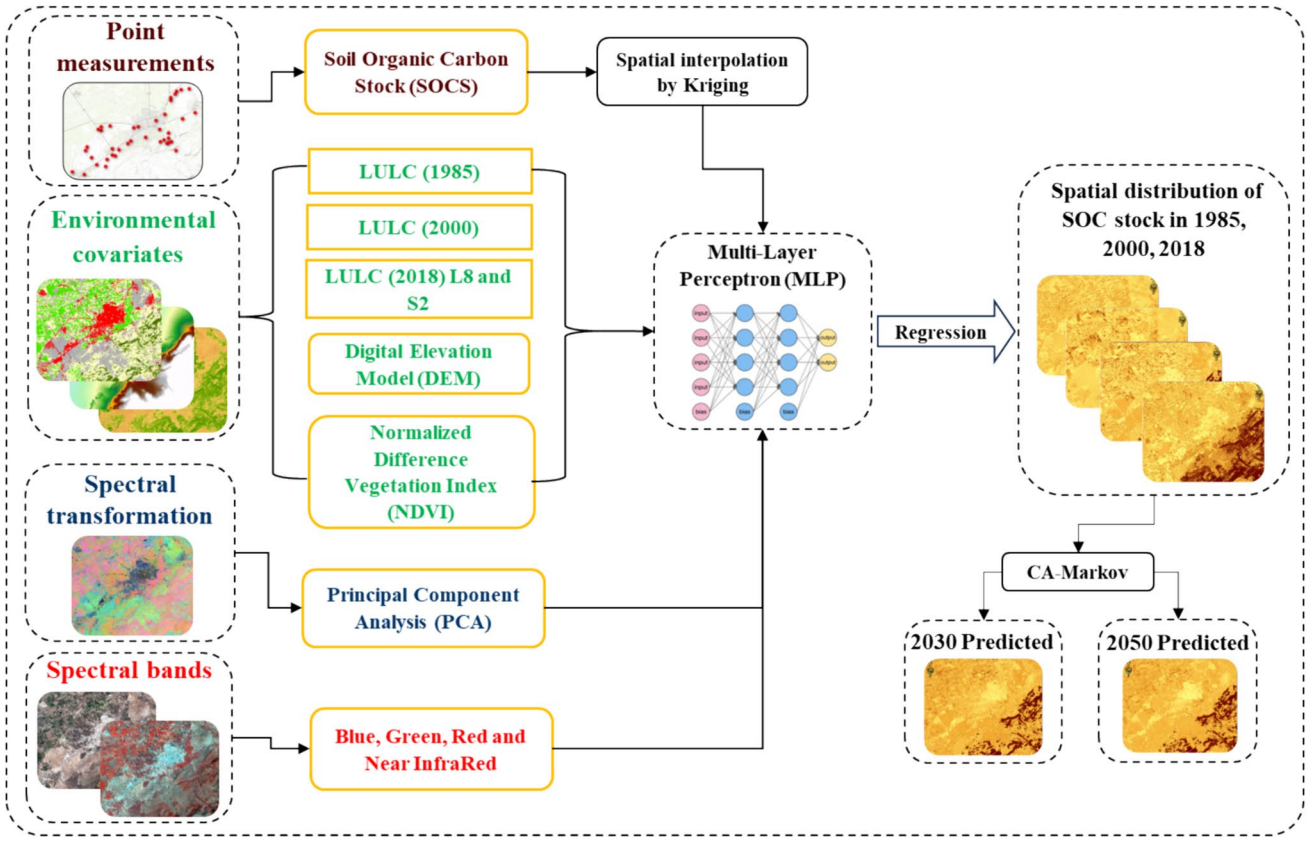

Fig. 4 Prediction of the spatiotemporal SOCS evolution (1985–2050) by modelling using MLP and CA-Markov models

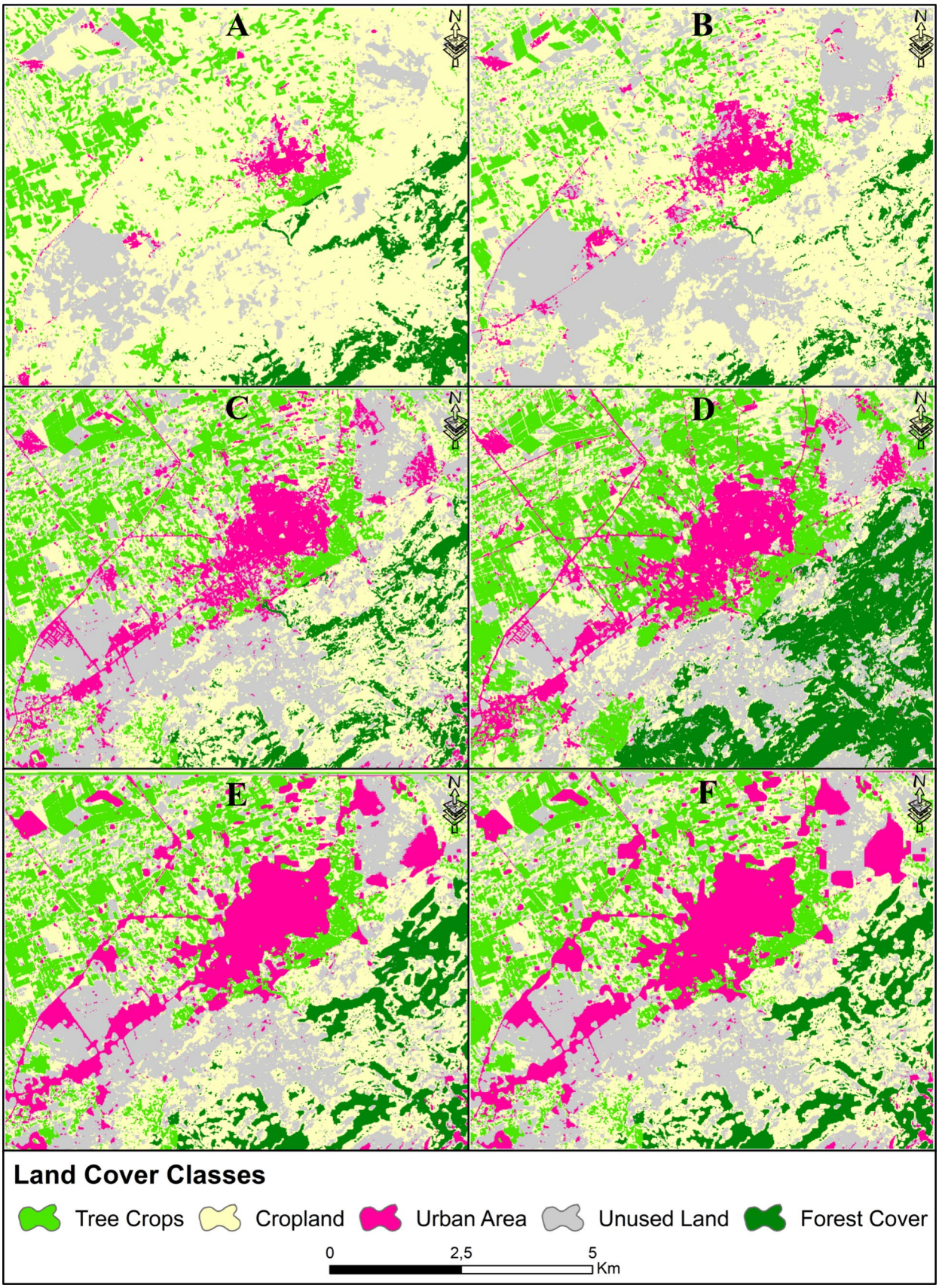
A
B
C
D
E
F
N
Land Cover Classes
Tree Crops
Cropland
Urban Area
Unused Land
Forest Cover
0
2,5
5
Km

◂**Fig. 5** LULC maps for years: **A** 1985 Landsat 5 TM, **B** 2000 Landsat 5 TM, **C** 2018 Landsat 8 OLI, **D** 2018 Sentinel-2 MSI, **E** predicted for 2030, and **F** predicted for 2050, derived from Landsat 5 TM/8 OLI images

areas, and forest cover) were considered to assess the accuracy of the 2018 mapping results from each satellite using the SAM-supervised classification method. This made it possible to check and compare the performance of the algorithm in its ability to classify the 5 LULC units from Landsat-8 OLI and Sentinel-2 MSI data. The accuracy of the land cover maps in this study is calculated using the overall accuracy (OA), which measures the proportion of ground control points in each LULC type that are correctly classified in relation to the total number of points in the LULC map. The OA obtained from this assessment quantifies the accuracy of the LULC classification. This accuracy is calculated from the following equation (Eq. 5) proposed by [68]:

$$\text{OA of LULC}[\%] = \frac{\text{Ground control points correctly classified}}{\text{Total number of Ground control points}} \times 100. \quad (5)$$

To evaluate the predicted SOCS maps for 2018 modelled by the ANN perceptron MLP model from Landsat 8 OLI (30 m) and Sentinel-2 MSI (10 m) satellite images, we used the 40 points sampled in this study to measure SOCS in each LULC type as reference data. Using these 40 points, we extracted the predicted SOCS values for each point and then defined three intervals: (4.36–6.79), (6.79–9.22) and (9.22–11.66). We assessed whether the two values (actual and predicted) of a point fell within one of these intervals. If this was the case, we assigned the values "TRUE"; otherwise, "FALSE". Using this method, we calculated the overall accuracy of the predicted SOCS values for each LULC type, as well as the overall accuracy of the predicted SOCS map. The accuracy of the predicted SOCS maps in this study is measured based on the overall accuracy, which evaluates the proportion of points with the TRUE value in relation to the total number of points (Eq. (6) proposed in this study). The evaluation of the predicted SOCS maps is of crucial interest for validating and guaranteeing the reliability of the MLP deep learning model used to estimate SOCS from Landsat 8 OLI and Sentinel-2 MSI satellite data. This evaluation also enables us to check whether the spatial resolution of the input data impacts the spatial modelling of the SOCS.

$$\text{OA of SOCS}[\%] = \frac{\text{number of points with the value}\varepsilon\text{TRUE}\varepsilon}{\text{Total number of sampling points}} \times 100. \quad (6)$$

Results

Analysis of the Historical and Projected LULC Dynamics

The current and projected spatiotemporal dynamics of the LULC classification schemes are presented in Fig. 5. The analysis focused on the main spatial units, which include cropland (yellow colour), unused land (dark sand colour), forest cover (dark green colour), urban areas (red colour) and tree crops (green colour). A comparison of the initial state (Fig. 5A), which represents the spatial distribution of land-use units in 1985, and the predictive geo-simulation for 2050 (Fig. 5F) using CA-Markov shows significant changes for all LULC units. Spatially, the spatial distribution of agricultural land was very dominant in 1985 and 2000, but a significant and gradual reduction was observed from 2018 to 2050. A similar and relatively less significant regressive trend is observed in forest cover, as shown by the distribution of forest cover in 1985 and the projected distribution for 2050.

It should also be noted that the comparative analysis of the distribution of LULC classes in 2018 using the Landsat 8 OLI sensor (Map C) and Sentinel-2 MSI (Map D) shows a significant contribution from the use of 10 m high spatial resolution data in the classification of LULC units. The improved classification using Sentinel-2 MSI compared with Landsat 8 OLI is supported by a better estimate of the spatial distribution of forest cover and the structures of urban areas, particularly road networks. For example, on Landsat 8 OLI Map C at 30 m spatial resolution, certain segments of the road network were not correctly classified, but the use of more precise Sentinel-2 MSI data at 10 m resolution enabled better distinction between LULC classes. Similarly, this comparative analysis shows that the use of Sentinel-2 MSI enabled certain confusions between cropland and forest areas observed in the classification of the map resulting from the classification of Landsat 8 OLI multispectral data to be correctly discriminated. The visual analysis may suggest an overestimation of the distribution of forest cover in map D, but this is closely linked to a significant gain in forest-class pixels, which have been classified as farmland, indicated by the yellow colour in the legend. However, regardless of this qualitative distinction between unused land, areas of tree crops and areas of natural forests, the spatial distributions of these three types of LULC have undergone increasing changes over the period from 1985 to 2050.

Conversely, progressive changes have been observed in the distribution of urban areas, which correspond to the red colour in the legend. The intensity of change in urban areas is clearly the greatest of all the forms of LULC in the study area over the period from 1985 to 2018 and according to the projections for 2030 and 2050. Indeed, the analysis of the

initial state (1985) suggests a very small proportion of urban areas that are visibly very localised. However, the extent and characteristics of the spatial distribution of urban areas have changed significantly and could become the most dominant spatial unit in terms of spatial extent by 2050. The impact and spatiotemporal interrelationships of these changes in the spatial distribution of LULC units on the productive properties of the region's soils, particularly their carbon content, are addressed in this analysis.

From a statistical point of view (Table 3 and Fig. 6), the results obtained confirm the abovementioned cartographic observations of LULC. Based on the situation at the initial date (1985) and future projections (2050), the proportions of the spatial distribution of LULC units could increase from 11.6% (29.3 km^2) to 18.2% (46 km^2) for tree crops; 68.9% (173.7 km^2) to 33.9% (85.5 km^2) for cropland; 1.8% (4.5 km^2) to 16.3% (41.1 km^2) for urban areas; 11.3% (28.5 km^2) to 23.5% (59.2 km^2) for unused land and from 6.4% (16.2 km^2) to 8.2% (20.7 km^2) for natural forest cover. These changes in the spatial distribution of LULC units are both regressive for agricultural land and significantly progressive for other LULC units.

However, the greatest rate of positive change is in the spatial extension of urban areas, with an increase of 15.5% by 2050. The rates of positive change are relatively low for unused land and tree-growing areas, at +12.2% and +6.6%, respectively. These results highlight the importance of growing urbanisation in the Béni-Mellal area to the detriment of other forms of LULC, with a -35% reduction in cropland by 2050. A comparative analysis of area gains and losses shows that the dynamic of changes in conversions between LULC units continues to be to the disadvantage of agricultural land, which is gradually being reduced in favour of urban areas and unused land. On the other hand, the exceptional increase in tree crops observed is linked to new agricultural development policies introduced since the launch of the Moroccan Ministry of Agriculture's support programme for the tree sector (Green Morocco Plan). The direct effect of this new regulatory framework has been major reforms to the state and community land tenure system, which have enabled new land to be developed for arboriculture.

Furthermore, as observed in the visual analysis of the LULC maps, the classification statistics of the two sensors Landsat 8 OLI and Sentinel-2 MSI for the LULC mapping of 2018 highlighted the discrepancies in the accuracy of the statistical estimates between the results from the two sensors. This was clearly significant for two LULC units, namely, the proportion of forest cover estimated at 6.8% according to the results of the classification of Landsat 8 OLI images, whereas the statistics from the results of the classification of Sentinel-2 MSI images suggested a proportion of 17.5%, i.e., a difference of 10.7%. The same is true for the cropland statistics, which were estimated at 37.6% using 30 m multispectral images (Landsat 8 OLI) and 24.6% using 10 m multispectral images (Sentinel-2 MSI), i.e., an estimated difference of 13.1%. These results suggest that the image classifier used (SAM) was not able to discriminate all the spectral similarities between natural forests and

Table 3 Change in surface area in the different LULC categories between 1985 and 2050 for Landsat 5 TM/8 OLI and 2018 for Sentinel-2 MSI

Type of LULC	Area (Km^2)					
	1985		2000		2018 (Landsat 8 OLI)	
	(km^2)	(%)	(km^2)	(%)	(km^2)	(%)
Tree crops	29.3	11.6	23.2	9.2	45.5	18
Cropland	173.7	68.9	139.4	55.3	95	37.6
Urban area	4.5	1.8	11.6	4.6	27.1	10.7
Unused land	28.5	11.3	67.5	26.8	67.8	26.9
Forest cover	16.2	6.4	10.5	4.2	17.1	6.8
Total	252.2	100	252.2	100	252.5	100
Type of LULC	Area (Km^2)					
	2018 (Sentinel-2 MSI)		Prediction 2030		Prediction 2050	
	(km^2)	(%)	(km^2)	(%)	(km^2)	(%)
Tree crops	59.4	23.5	46	18.2	46	18.2
Cropland	62.1	24.6	86.4	34.2	85.5	33.9
Urban area	30.7	12.1	36.6	14.5	41.1	16.3
Unused land	56.4	22.3	61.7	24.4	59.2	23.5
Forest cover	44.1	17.5	21.8	8.6	20.7	8.2
Total	252.7	100	252.5	100	252.5	100

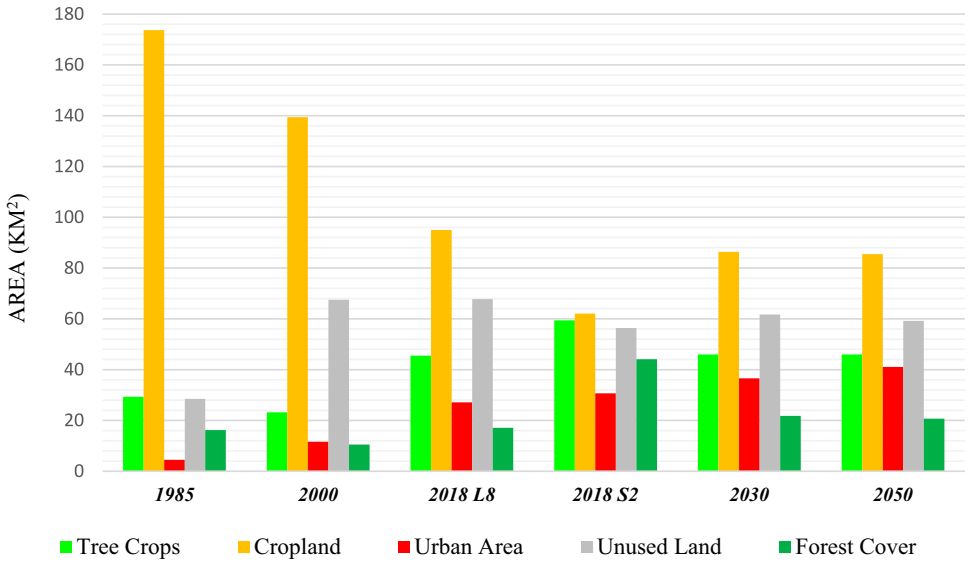

Fig. 6 Change evolution in surface area in km^2 for the different LULC unit categories from 1985 to 2050.

cropland when using the 30 m resolution images and that this was possible when using the 10 m resolution multispectral images. For these reasons relating to the precision of the quality of the classification, the statistics provided remain indicative but have nevertheless made it possible to identify the main trends characterising the evolution of intraclass transitions in the Béni-Mellal region.

Soil Organic Carbon Contents, Stocks, and Soil Texture of each LULC Type

Figure 7 presents a comparative analysis of the quantitative distribution of the soil organic carbon (SOC) content and soil organic carbon stock (SOCS) of the samples as a function of the textural characteristics of the soils in the different LULC units at a depth of 15 cm. This result shows a wide variation in the minimum, maximum and median statistical indicators of the parameters analysed between LULC classes and even within the same LULC class.

The percentage content and rate of variation of organic carbon content in tree crop soils was the lowest (between 3.9 and 5%). Very similar statistical proportions were observed in the SOC distribution of cropland and unused soil, with respective rates of variation of approximately 3.8 to 5.5% and 4.1 to 5.8%. However, both the percentage content and the rate of change of SOC are higher in forested areas, ranging from 7.5 to 10.2%, i.e. approximately three times higher than in cropland. In urban areas, SOC contents ranging from 3.8 % to 6% were observed, which were slightly higher than those in cropland. Similarly, if we focus on the median values of SOC content, the differences are much more marked. Except for the median values for cropland, which are clearly

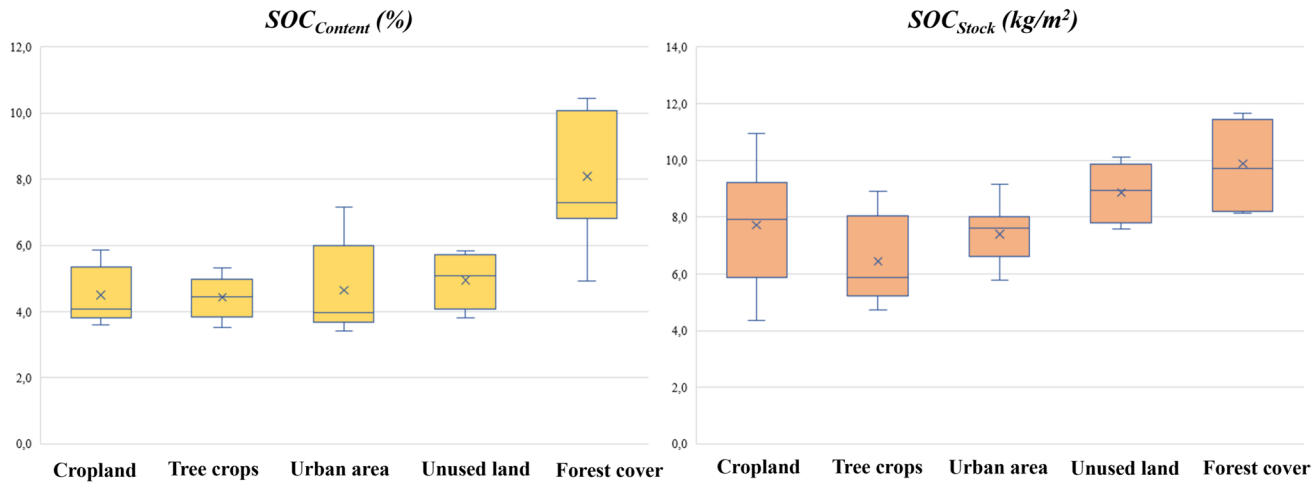

Fig. 7 Measured $SOC_{Content}$ (left) and SOC_{Stock} (right) of the soils sampled in the different LULC types (reference: [51])

very close to those for urban areas (approximately 4%), the median value for forest cover is 7.2%.

On the other hand, the comparative analysis of SOCS suggests much less marked differences than when focusing on SOC. For example, SOCS values ranged from 8.1 to 11.7 kg/m^2 in forest class soils compared with 4.7 to 8.9 kg/m^2 in tree crop soils, which had the lowest SOCS values. The variation in SOCS values in the other LULC units was as follows: 5.8 to 10.1 kg/m^2 in agricultural soils, 5.8 to 9.2 kg/m^2 in urban soils and between 7.6 and 10.1 kg/m^2 in unused land.

Based on the median SOCS values of the samples analysed, the SOCS is highest in forest soils, with an average of 9.9 kg/m^2, followed closely by the SOCS of unused land, with an average of 8.9 kg/m^2, i.e. a unit difference of 1 kg/m^2. The median SOCS of cultivated land is 7.9 kg/m^2, which is very similar to the median SOCS of soils in urban areas, which is 7.4 kg/m^2, a difference of 0.5 kg/m^2. Finally, of the five types of LULC, the SOCS of tree crops is the lowest, with a median value of 6.4 kg/m^2. This trend could be explained by the maintenance practices applied to tree crop soils, which appear to reduce the stock of litter and organic matter on the surface.

Statistical Analysis of the SOCS Distribution from 1985 to 2050 per LULC Unit

Multidate statistics of SOC stock distribution by LULC type were produced by considering mean SOCS values and LULC class areas. The results obtained (Table 4 and Fig. 8) show significant changes in the SOC stock of LULC units over the reference period from 1985 to 2018. The same applies to the results of the predictive geo-simulations for the period 2018 to 2050. Considering the results from Landsat 5 TM for 1985 and Landsat 8 OLI for 2018, the most significant positive changes were observed in the SOC stock of tree crop soils, i.e., a change of 103.7 kg.10^6 over the period from 1985 to 2018. Nevertheless, the results of projections to 2050 suggest that we should expect a gradual decline in the SOC stock in tree crop soils in the long term. This can be explained by a low rate of positive change in the SOC stock in tree crop soils of approximately 3.2 kg.10^6 between 2018 and 2050, much lower than that observed over the period 1985 to 2018.

However, the opposite situation is observed in the SOC stock of cultivated land soils, which are characterised by the highest rate of negative change of − 606 kg.10^6 over the period 1985 to 2018 and − 73.1 kg.10^6 in 2050. At the same time, positive changes in the SOC stock of 349.7 kg.10^6 were observed in the soils of uncultivated land over the period from 1985 to 2018. However, the results of predictive geo-simulations with CA-Markov suggest a long-term (2050) decline in the SOC stock of − 76.5 kg.10^6. On the other hand, positive variations in SOCS were observed in forests, resulting in positive rates of change of 8.9 kg.10^6 (1985 to 2018), 46.5 kg.10^6 (2018–2030) and 35.6 kg.10^6 (2018–2050). Positive variations were also observed in urban soils of 167.2 kg.106 (1985 to 2018), 70.3 kg.10^6 (2018–2030) and 103.6 kg.10^6 (2018–2050). This shows that the spatial distribution of SOCS and its temporal dynamics in terms of positive and negative variations are strongly linked to spatiotemporal changes in land occupation and use.

Spatiotemporal Prediction and Mapping of SOC Stocks

Figure 9 shows the results of quantitative mapping of the spatial and temporal distribution of SOC according to the underlying dynamics of land use, land cover and

Table 4 Change in SOCS by LULC type between 1985, 2000, 2018, 2030 and 2050 for Landsat 5 TM/8 OLI and 2018 for Sentinel-2 MSI

Type of LULC	Total SOCS (kg.10^6)					
	1985	2000	2018 Landsat 8 OLI	2018 Sentinel-2 MSI	2030	2050
Tree crops	187.5	148.5	291.2	380.16	294.4	294.4
Cropland	1337.5	1073.4	731.5	478.17	665.3	658.4
Urban area	33.3	85.8	200.5	227.18	270.8	304.1
Unused land	253.7	600.8	603.4	501.96	549.1	526.9
Forest cover	160.4	104	169.3	436.59	215.8	204.9

Type of LULC	SOCS change (kg.10^6) Landsat 5 TM/8 OLI		
	1985–2018	2018–2030	2018–2050
Tree crops	103.7	3.2	3.2
Cropland	− 606	− 66.2	− 73.1
Urban area	167.2	70.3	103.6
Unused land	349.7	− 54.3	− 76.5
Forest cover	8.9	46.5	35.6

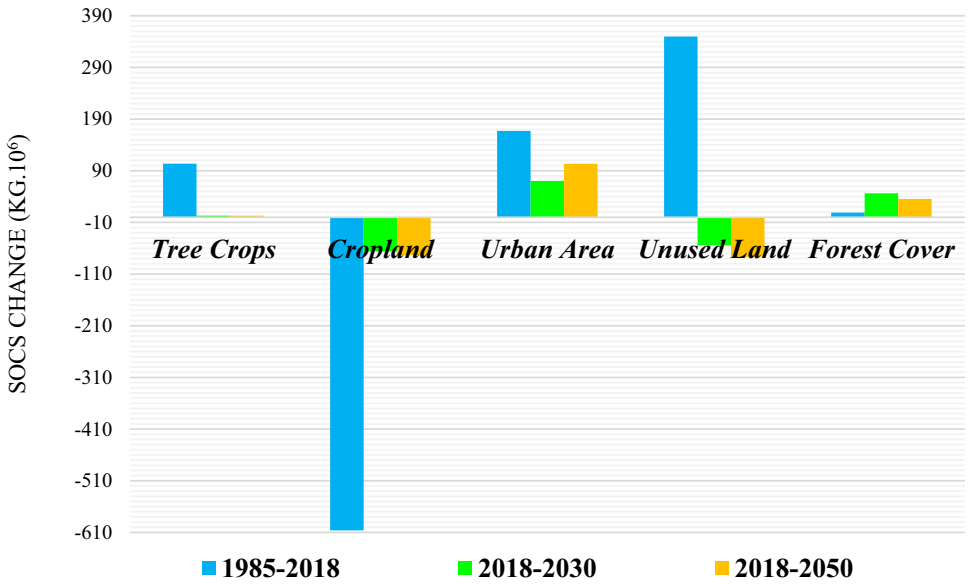

Fig. 8 Gain/loss (kg.10^6) of SOCS change by LULC class for the periods of 1985, 2018, 2030 and 2050 based on Landsat 5 TM/8 OLI data

environmental variables. The dynamics of the spatial and temporal distribution of topsoil SOC stocks (0 to 15 cm) show considerable spatial variability over the period from 1985 to 2050. The SOC stock maps obtained by spatial regression using deep learning (MLP) trained with ten predictor variables were used to map six classes of SOCS quantities across the study area. In all six maps, the highest values (10.4 to 11.5 kg/m^2) are visibly concentrated in the southeast, mainly in forested areas, and the lowest values (4.6 to 5.8 kg/m^2) are towards the centre in urban areas. The intermediate values, on the other hand, have a more heterogeneous spatial distribution for all dates, which can be linked to the characteristics of the spatial distribution of the other LULC classes and the environmental covariates.

However, despite the similar spatial distribution in the six maps, several trends should be highlighted based on multidate dynamics and predictive geo-simulations. In forest soils in particular, the spatial distribution of the SOC stock is visibly very variable according to the years 1985, 2000, 2018 and 2050, but it is progressively characterised by a slight spatial extension. Exceptionally, the Landsat 5 TM result (map B from 2000) showed a slight extension of the spatial distribution of high SOCS values. This could be explained by an underestimation of the distribution of forest cover in the LULC classification generated using Landsat 5 TM multispectral images and by the mediocre quality of the covariate data (spectral indices) for the same date for the predictive spatial modelling of SOCS. These data-related characteristics are likely to affect the predictive performance of the MLP model used for the spatial prediction of the SOC stock. This argument is supported by the fact that the result (map D) of the same algorithm and for the same covariates as predictors of the SOCS distribution in 2018 based on Sentinel-2 MSI data (map D) indicated a greater extension of high SOCS values than that in 2018 based on Landsat 8 OLI data (map C). Thus, it is concluded that the data quality and spatial resolution are important characteristics for spatial modelling of the SOCS distribution with deep learning models.

Thus, spatial autocorrelation analyses were carried out to gain a better understanding of the main factors influencing the spatial distribution of SOCS. Figure 10 provides a comparison of the spatial correlations of environmental covariates (spectral indices), image transformation (PCA), land use and land cover, DEM, and spectral bands with respect to the spatial distribution of SOCS in 2018 based on Landsat 8 OLI and Sentinel-2 MSI results. Irrespective of the satellite sensor used, the spatial autocorrelation results suggest that the spatial distribution of LULC units, topography (DEM) and environmental factors (NDVI) are the main factors influencing the quantitative distribution of SOCS in the study area. However, for the factor linked to the spatial distribution of LULC units, the comparative analysis of this result highlights a significant contribution from the use of Sentinel-2 MSI multispectral images compared with Landsat 8 OLI multispectral images. Indeed, as observed on the maps of the SOCS distribution, the LULC of the Sentinel-2 MSI image classification has a correlation of R = 0.8, which is clearly higher than that obtained between the SOCS distribution and the LULC of the Landsat 8 OLI classification, which is R = 0.63. This shows that the use of images with a high spatial resolution of 10 m has enabled a better estimation of the spatial distribution of LULC units and an improvement in the spatial modelling of SOCS with the MLP algorithm, which can be explained by a gain of approximately R = 0.2 with the use of Sentinel-2 MSI images. Nevertheless, for the

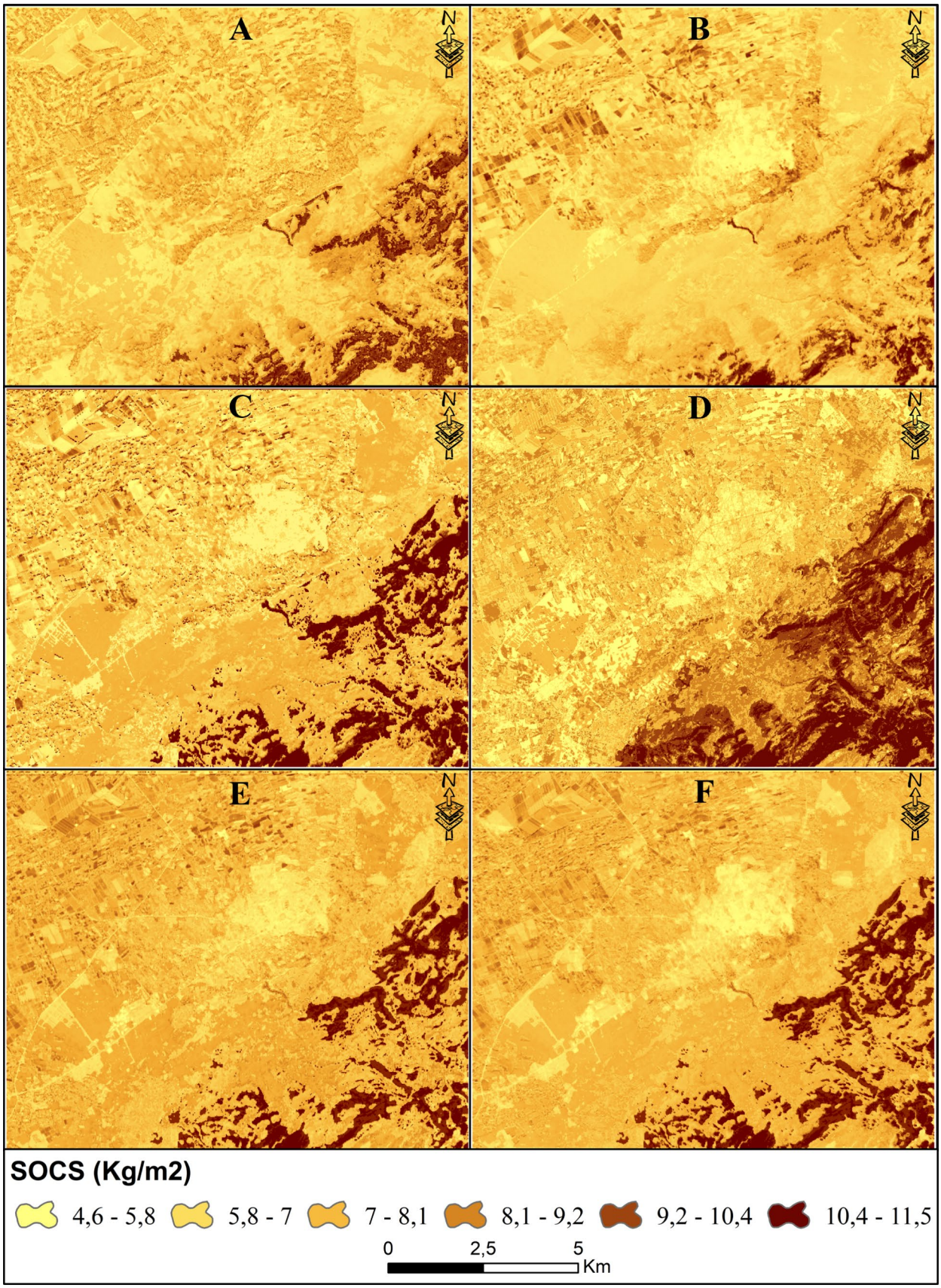
A
B
C
D
E
F
N
SOCS (Kg/m2)
4,6 - 5,8
5,8 - 7
7 - 8,1
8,1 - 9,2
9,2 - 10,4
10,4 - 11,5
0
2,5
5
Km

◂**Fig. 9** Spatiotemporal prediction of soil organic carbon stocks (in kg/m^2) maps for **A** 1985 Landsat 5 TM, **B** 2000 Landsat 5 TM, **C** 2018 Landsat 8 OLI, **D** 2018 Sentinel-2 MSI, **E** 2030, and **F** 2050, predicted from Landsat 5 TM/8 OLI images

other variables, we can see that the Landsat 8 OLI NDVI has a very high positive spatial correlation with the SOCS and is higher than that of the Sentinel-2 MSI NDVI, with R = 0.94 and R = 0.65, respectively, i.e. a difference of 0.29. This is observed with only a few differences for the other covariates, except for the DEM. This leads us to conclude that the use of Sentinel-2 MSI multispectral images was beneficial only for improving the classification of LULC units and that the predictive performance of the depth learning model (MLP) used is only slightly sensitive to the improvement in spatial resolution.

Analysis of Soil Textural Properties

Soil texture is one of the properties that determine the mineralogical and functional characteristics of soil. It provides information on the relative abundance of particle sizes of soil constituents and therefore plays a significant role in a soil's capacity to store and/or leach organic soil components. Figure 11 shows the results of analyses of the textural characteristics of soils (sand (%), clay (%), and silt (%)) in the study area for the five main LULC classes. The results show that the relative proportions of the three elements that define soil texture, i.e. the proportion of clay, sand, and silt, vary significantly from one LULC unit to another. In urban areas, the maximum proportions obtained were 40% sand, 52% silt and 38% clay, with median proportions of 30%, 40% and 30%, respectively. On the other hand, in the soils of forest areas, the maximum proportions obtained are 20% sand, 50% silt and 30% clay, and their median proportions are 20%, 50% and 30%, respectively. These median proportions, which are identical to the maximum proportions, show that the textural characteristics of forest soils are particularly homogeneous, unlike the soils of the other LULC units. This also reflects the characteristics of soils that are sufficiently developed and deep.

On the other hand, in the other LULC units, except for the proportion of silt in the soils of cultivated land, the relative proportions of clay, silt and sand in the soils of unused land, tree crops and cropland are characterised by a wide dispersion of values in relation to the median values. In cropland soils, for example, the proportion of sand is 20%, silt is 49% and clay is 43%, with median values of 20%, 50% and 37%, respectively. Similarly, the textural characteristics of arboriculture soils are comparable to those of farmland soils. The maximum proportions of tree crop soils are 33% sand, 50% silt and 32% clay, with median values of 28%, 49% and 41%, respectively. For soils from unutilised land, the maximum proportions are 25% sand, 50% silt and 40% clay, with median values of 18%, 38% and 41%, respectively. These slight differences in the textural characteristics of the soils of the croplands, orchards and unused land could largely explain the minor differences observed in the SOCS for these same LULC units.

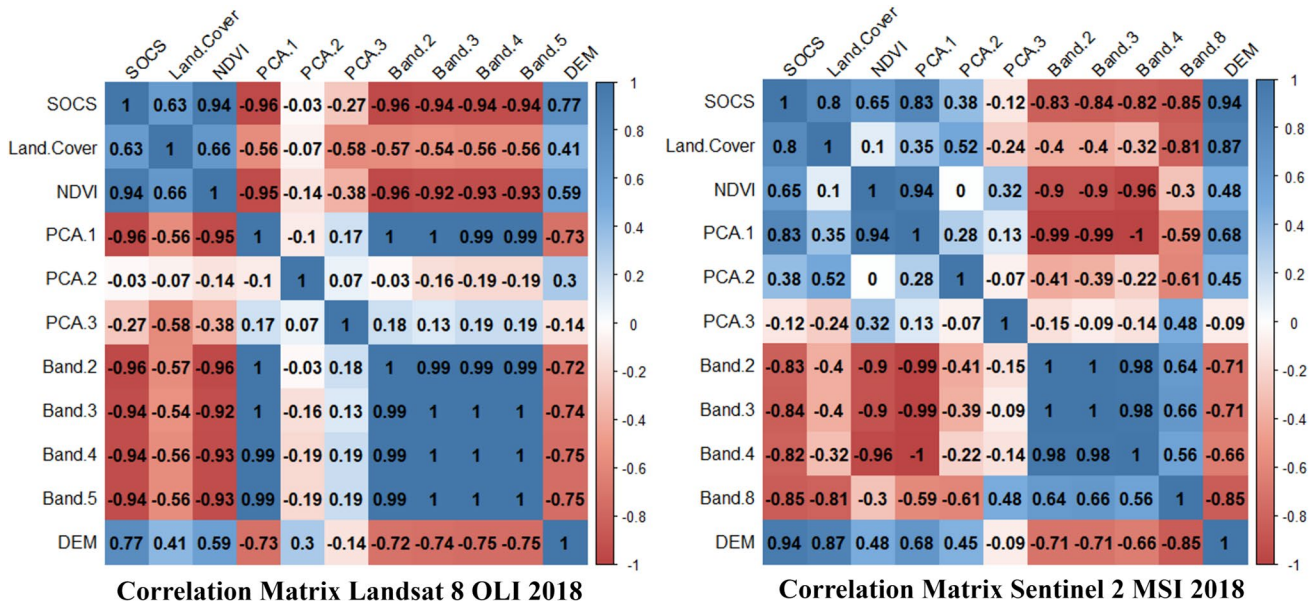

Fig. 10 Comparison of correlation matrices between soil organic carbon stock predicted using MLP, environmental covariates, PCA and spectral bands from Landsat 8 OLI (left) and Sentinel-2 MSI (right) images for 2018

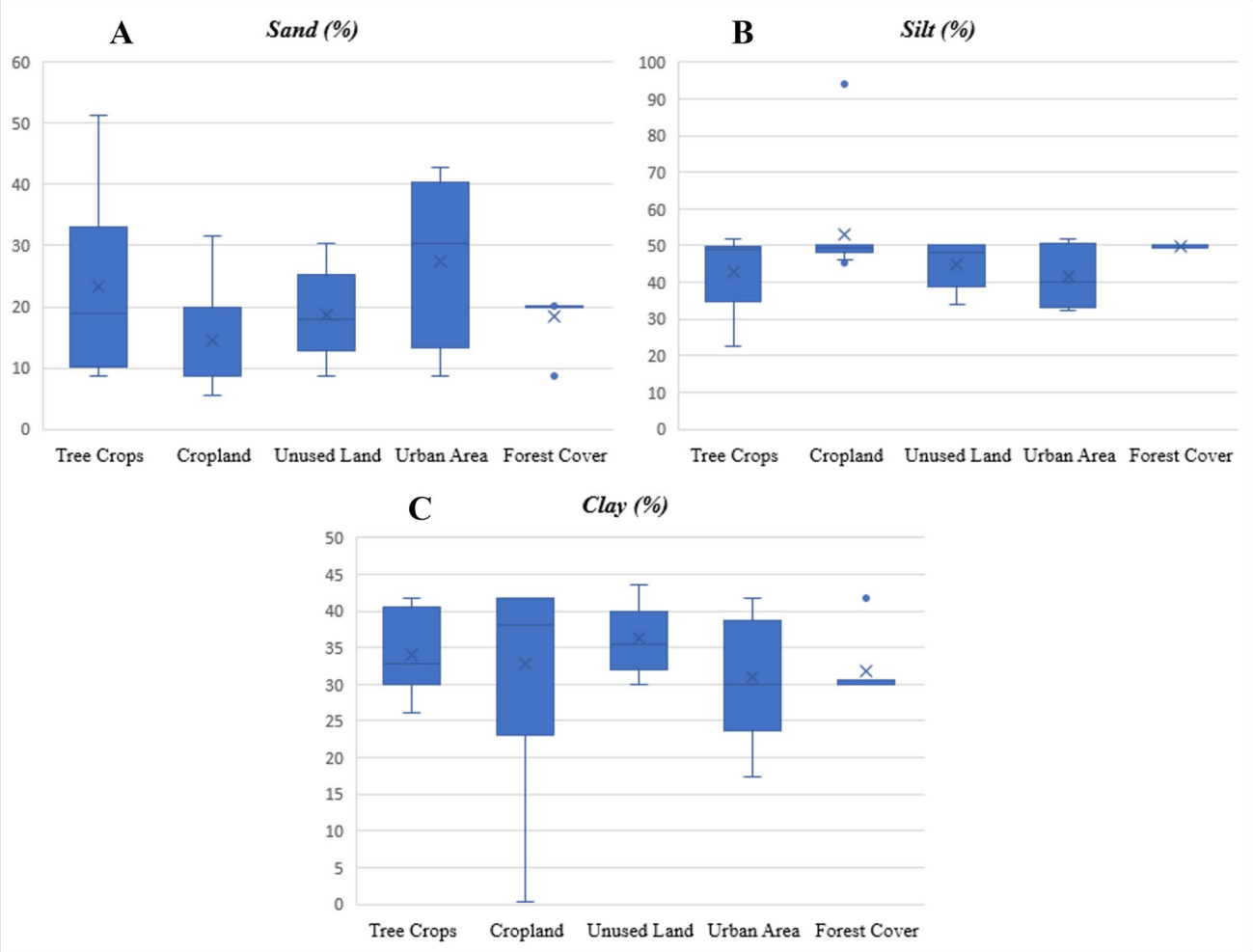

Fig. 11 Variation in **A** sand, **B** silt, and **C** clay percentages by LULC type (reference: [51])

Overall Accuracy and Uncertainty Assessment

Table 5 presents a comparative analysis of the overall accuracy (OA) of LULC unit classification and SOCS spatial modelling based on Landsat 8 OLI and Sentinel-2 MSI sensors for 2018. The result shows a significant difference between the accuracy of the LULC unit classification results for Sentinel-2 MSI and Landsat 8 OLI data. However, the accuracy of SOCS spatial modelling does not reveal significant differences. For image classification, the overall accuracy of the result from Sentinel-2 MSI is 88%, i.e. an improvement of 10% compared with the result from Landsat 8 OLI multispectral image classification (OA = 78%). An analysis of the accuracy by LULC class shows that using Sentinel-2 MSI data with a better spatial resolution of 10 m resulted in 100% detection of built-up areas. On the other hand, with an accuracy of 70%, the use of Landsat 8 OLI images did not result in better detection and classification of built-up areas. The same applies to the accuracy of the cultivated land class, which is 60% for the Landsat 8 OLI results, whereas the accuracy of the cultivated land class reaches 90% with the Sentinel-2 MSI result. Overall, the global and LULC class accuracies suggest a clear improvement in the classification of LULC units using Sentinel-2 MSI high spatial resolution images compared with Landsat 8 OLI. However, when the accuracy of the spatial modelling of SOCS is analysed comparatively, there are no significant differences between the results from the two sensors. The overall accuracy of SOCS spatial modelling using Sentinel-2 MSI data is 55.57%, and that using Landsat 8 OLI data is 50.89%, i.e. a difference of 4.68%. However, for both sensors, the highest accuracy of the SOCS distribution was obtained for the unused land class (77.77%), and the lowest accuracy was obtained for the tree crop class (37.5% for Sentinel-2 MSI and 37.5% for Landsat 8 OLI). Finally, the comparative accuracy analysis between the two sensors reveals that the accuracy of SOCS spatial modelling via deep learning regression with MLP is only slightly improved by

Table 5 Evaluation of the overall accuracy and uncertainty of LULC maps and the SOCS prediction model using Landsat 8 OLI and Sentinel-2 MSI images for 2018

Type of LULC	LULC maps		SOCS maps	
	Sentinel-2 MSI	Landsat 8 OLI	Sentinel-2 MSI	Landsat 8 OLI
Tree crops	90%	80%	37.5%	37.5%
Urban area	100%	70%	60%	60%
Cropland	90%	60%	45.45%	36.36%
Unused land	70%	80%	77.77%	77.77%
Forest cover	90%	100%	57.14%	42.85%
Total	88%	78%	55.57%	50.89%

using data with a high spatial resolution. On the other hand, the performance of the SAM classifier for detecting and classifying the LULC units used improved significantly using Sentinel-2 MSI multispectral images of 10 m (Table 5).

Discussions

Quantitative spatial modelling and predictive geo-simulations of SOCS are of crucial importance for land-use planning applications aimed at carbon sequestration in the land−plant system. Based on soil sample analysis data, it has been demonstrated in several evidence-based studies that the spatial variability of SOCS can be modelled via spatial integration of environmental covariates, land use change, soil characteristics, and topography via machine learning [26, 27], deep learning [17] and/or multivariate geostatistical methods [24]. Within the framework of this study, a multidate (1985, 2000, 2018, 2030, 2050) and multi-sensor (Landsat 5 TM/8 OLI and Sentinel-2 MSI images) deep learning approach was used to quantitatively evaluate the evolution of the spatial distribution of the SOCS of the Béni-Mellal region and its future changes by 2050.

The results of the spatial regression with MLP suggest a spatial distribution of SOCS that is consistent with the multidate dynamics of the distribution of LULC units. Nevertheless, relatively significant differences were observed in the rates of change in SOCS according to the different types of LULC. Contrary to what might be expected, by analysing the historical (1985 to 2018) and future (2018 to 2050) dynamics, positive rates of change were found in the organic carbon stock of forest soils. The SOCS in forest soils is expected to reach 204.9 kg.10^6 in 2050, whereas it was estimated at 160.4 kg.10^6 in 1985, i.e. a rate of positive change of 35.6 kg.106. This increase in SOCS in forest soils is linked to several forest management actions carried out as part of the National Watershed Management Plan launched in 1996 by the High Commission for Water, Forests, and the Fight against Desertification in Morocco, which focused on forest reforestation and the planting of fruit trees. The effect of these management actions has been to improve the sequestration of organic carbon by forests, particularly through the introduction of new species that are more resistant to drought. In addition, the protective function of forests against soil erosion is a feature that significantly reduces the leaching of organic matter from the surface layer (0 to 15 cm). In addition, wooded areas such as forest ecosystems have a high carbon sequestration potential linked to the continuous fall of litter and its accelerated metabolism [69,70]. These functional characteristics of forests could explain why we found that the SOCS concentration was significantly higher in forests than in other LULC units. Comparative analyses of soil textures according to LULC units showed forest soils with a higher silt content (50%) and a very low sand content (20%) than soils in other LULC classes. These physical properties that characterise forest soils in this zone are also factors that can favour better accumulation of organic carbon in forest soils. Indeed, it has been noted in several previous studies that forest soils have a greater potential for sequestering and storing organic carbon than soils from other forms of land use or occupation [71, 72]. However, it should be pointed out that [17] found in South Africa that the SOCS concentration was higher in grasslands (SOCS max = 87.44 t/h) than in other LULCs, which include natural forests, commercial forests, infertile land, shrubs, and urban vegetation.

Furthermore, the study shows that significant negative rates of change of approximately − 73.1 kg.10^6 could occur in the SOCS of cultivated land soils by 2050. This regressive trend in SOCS in farmland can be explained by the intensification of farming practices in the region, particularly the mechanisation of ploughing and the application of inorganic fertilisers, which would increase the rate of decomposition of soil organic matter. In fact, agricultural practices such as ploughing, which was once a manual activity with little capacity to stir up the soil, is now an activity that involves the use of large machines with a great capacity to plough the soil deeper. Intensive, deep ploughing accelerates soil erosion [2, 73], and the use of inorganic fertilisers leads to rapid decomposition of organic carbon in the soil. Thus, if the same rate of intensification and extension of agricultural land continues, the agricultural sector could result in an enormous loss of surface organic matter to a lower horizon and an increase in leaching by erosion. According to

[74], the type of land use or a change that disturbs it the least contributes to SOCS accumulation improvement, and conversely, intensive disturbances lead to significant losses and low absorption. For example, it has been shown that American soils have lost between 30 and 50% of the SOCS they contained before they were put to agricultural use, and this has been attributed essentially to the use of the plough to plough the soil [75, 76]. Several other researchers support the idea that reduced tillage is a practice that favours the storage of SOC in the topsoil and reduces its loss in the upper layers [76, 77]. The results of future geo-simulations using CA-Markov suggest that cultivated land will reach 33.9% of the total surface area of the study area over the next thirty years. This could result in a significant loss of total soil organic carbon stock in the Béni-Mellal region due to intensive agriculture.

However, the positive change in tree-growing land from 29.3 km^2 in 1985 to 46 km^2 in 2050, i.e. a positive rate of change of 18.2%, could be in favour of a good accumulation of carbon in tree-growing soils, contrary to the opposite situation linked to the increase in cropland areas. The results obtained revealed a significant increase in the rates of positive change in tree crop soils, reaching 103.7 $kg.10^6$ between 1985 and 2018. This suggests that it is possible to assert that the conversion of land use to tree crops has a positive effect on soil organic carbon storage. In fact, in arboriculture agrosystems, certain agricultural practices, particularly deep ploughing, are used sparingly, which reduces losses of soil organic matter in the surface layer of the soil and favours its storage in the topsoil. Several factual studies have shown that LULC types play a dominant role in influencing SOC content and stock because surface soil disturbance, litterfall and decomposition vary with LULC, resulting in a difference in SOCS depending on land use [17, 30, 67, 78, 79].

It is therefore important to understand the need for new land-use strategies for the effective implementation of greenhouse gas mitigation directives in the Béni-Mellal region. For example, an increase of 103.7 $kg.10^6$ in SOCS in tree crop soils was observed over the period from 1985 to 2018. This increase follows the planting of fruit trees in the plains as part of the Green Morocco Plan (GMP) strategy, which aims to convert unused land and unsuitable cultivated areas into tree-growing zones. This has helped to protect the soil and increase soil organic carbon stocks. Such land-use change initiatives and their targeted uses are essential for boosting the carbon sequestration potential of soils.

In addition, the spatial relationships between the SOCS distribution, LULC units, environmental covariates and topography were examined. They indicated very high spatial interrelationships between the spatial distribution of SOCS and LULC units, with a correlation of approximately 0.8. However, the resolution of multispectral images was found to be an important factor in the detection and spatial categorisation of pixels in the different LULC units but seems less important for the accuracy of the spatial modelling of SOCS. For example, it was found that the accuracy of classification of LULC units using Sentinel-2 MSI data is 88% compared with an accuracy of 78% using Landsat 8 OLI. However, very little difference was observed between the spatial modelling of SOCS using Sentinel-2 MSI data (OA = 55.57%) compared with an OA of 50.89% using Landsat 8 OLI. This suggests that the improvement in spatial resolution is clearly more beneficial for improving the classification of LULC units than for deep learning geo-spatialization of the SOC stock distribution.

Advantages, Disadvantages, and Limitations

See Table 6.

Conclusion

To quantitatively analyse the spatiotemporal evolution of SOCS in the Béni-Mellal region of Morocco, a multidate, multi-sensor approach and analyses of soil samples were used in this study. To this end, ten predictors, namely, environmental factors (NDVI, EVI, SAVI), land use and land cover changes, topography, spectral bands (RGB, NIRGB), principal component analysis, maximum noise fraction and soil samples (40 sites), were spatially integrated to train the deep learning model (MLP) to spatially model the SOCS distribution over the reference period covering the initial date (1985), intermediate date (2000) and recent date (2018). The cartographic and statistical analyses carried out over the period 1985–2018 show that the dynamics of the distribution of SOCS are closely linked to those of the LULC units, with rates of change that are both progressive in tree crop soils (103.7 $kg.10^6$), unused land (349.7 $kg.10^6$) and urban area soils (167.2 $kg.10^6$), slightly so in forest soils (8.9 $kg.10^6$) and significantly regressive in cropland soils (− 606 $kg.10^6$). However, from 2018 to 2050, the future dynamics of the SOCS spatial distribution assessed based on predictive geo-simulation using CA-Markov suggests a very significant positive evolution of SOCS in forest soils with a rate of change of 35.6 $kg.10^6$, while the regressive evolution in agricultural land should continue at − 73.1 $kg.10^6$ by 2050. Analysis of the spatial autocorrelations between the spatial distribution of SOCS and the predictors revealed that land use change and its uses, environmental characteristics and topography are the main factors impacting the spatial distribution of SOCS in the topsoil layer, with correlative relationships of 0.8, 0.94 and 0.94, respectively. However, it should be noted that the comparative accuracy analysis between the LULC unit classification results obtained from Sentinel-2 MSI and Landsat 8 OLI data shows that the use

Table 6 Critical evaluation of the advantages, disadvantages, and limitations of this study.

Advantages	Disadvantages	Limitations
Use of a multi-date, multi-sensor, multisource approach.	Lack of detail on predictor selection and model parameters (black box).	The study is based on 40 soil samples, which may not be representative of the entire study area. The limited sample size could influence the accuracy of the SOCS prediction over the whole study area.
Use of an advanced artificial intelligence ANN model (MLP), enhancing the predictive accuracy of the study.	No mention of data SOCS quality: absence of double-checking quality control measures.	Lack of scenarios for future prediction of LULC and SOCS limits the ability of the study to anticipate the possible ways of territorial evolution.
Integration of satellite data and soil samples for an in-depth and comprehensive analysis.	Limited exploration of the underlying mechanisms explaining the observed correlations, weakening the overall understanding of the processes studied (black box ANN/MLP model).	A more detailed discussion of model validation and sensitivity analysis is needed to strengthen the reliability of the results, highlighting the limitations and strengths of the model.
Demonstration of the strong link between SOCS dynamics and LULC changes.	Absence of integration of socio-economic factors influencing changes in LULC, restricting the scope of the analysis.	The lack of uncertainty and error analysis could limit the contributions of this research (reproducibility and robustness), not allowing a full assessment of the reliability of the predictions.
Use of geo-simulation to anticipate future changes in LULC and the SOCS, providing a forward-looking perspective.	Lack of in-depth evaluation of the performance of the MLP, the coefficient of determination R2, and comparison with other artificial intelligence ANN models, restraining the performance evaluation of the model.	The absence of other factors such as geology, climate or soil properties limits the model's ability to provide a more accurate spatial prediction of SOCS by not considering all relevant parameters.
Identification of the main factors influencing the distribution of the SOCS, contributing to an in-depth understanding of the processes.	Absence of use of advanced AI models (e.g. CNN) to classify LULC, which could improve the accuracy of the mapping.	The study did not examine the time lag between land use changes and SOCS variations, thus limiting the understanding of time lags and temporary responses in the system studied.
Comparative accuracy analysis between Sentinel-2 MSI and Landsat 8 OLI improves data reliability.	No sample and model all the horizons in the soil profile, limiting the analysis to the top 15 centimetres, which could result in an incomplete view of soil characteristics and their evolution.	The study is based on 40 soil samples, which may not be representative of the entire study area. The limited sample size could influence the accuracy of the SOCS prediction over the whole study area.

of 10 m spatial resolution data significantly improved the classification of LULC units with an accuracy of 88% compared with an accuracy of 78% for Landsat 8 OLI, i.e. a 10% improvement in terms of overall accuracy. However, there were no significant differences between the results from the two sensors in terms of the overall accuracy of SOCS spatial modelling, i.e. 55.57% accuracy for the result obtained using Sentinel-2 MSI data and 50.89% accuracy for the result obtained using Landsat 8 OLI data, i.e. a difference of 4.68%. This shows that the accuracy of spatial modelling of soil organic carbon stock using MLP deep learning regression is only slightly improved by using data with better spatial resolution. Finally, our results showed that the current spatial distribution and future evolution of the SOCS can be spatially modelled by artificial intelligence models (MLP, CA-Markov) using the results of sampling analyses, geo-environmental predictors, land use and land cover changes, topography, and spectral responses. However, this study did not address the time lag between the effects of land-use change and SOCS changes.

Acknowledgements We gratefully thank the Faculty of Science and Technology of Béni-Mellal, for having given us the means (transport and soil analysis laboratory) to carry out this work. We also like to thank Professor A. Barakat for his advice during the realisation of this study. Furthermore, we acknowledge support provided by the ECCOREV TOODS, MAMP-CNRS SOM, and CNES TOSCA TRISHNA projects.

Funding This work was supported by the ECCOREV TOODS, MAMP-CNRS SOM and CNES TOSCA TRISHNA projects.

Data availability The datasets used can be made available upon request from the corresponding author (M. Oukhattar).

Declarations

Conflict of interest All authors contributed to the production of the manuscript and declare no conflict of interest.

Consent to Publication This manuscript is an extension of the proceedings of GISTAM 2023: 9th International Conference on Theory, Applications and Management of Geographic Information Systems. It has not been submitted to, nor is it under review in, any other journal or publication venue.

References

1. FAO. Soil is a non-renewable resource. 2015.
2. Lal R. Soil carbon sequestration impacts on global climate change and food security. Science. 2005;304:1623–7.
3. Xiong X, Sabine GD, Brenton M, Wade R, Willie GH, Nicolas BC. Interaction effects of climate and land use/land cover change on soil organic carbon sequestration. Sci Total Environ. 2014;493:974–82.
4. Bernoux M, Conceicao MD, Carvalho S, Volkoff B, Cerri CC. CO_2 emission from mineral soils following land-cover change in Brazil. Glob Change Biol. 2001;7(7):779–87.
5. Hutchinson JJ, Campbell CA, Desjardins RL. Some perspectives on carbon sequestration in agriculture. Agric For Meteorol. 2007;142(24):1–302.
6. Yang RM, Zhang GL, Yang F, Zhi JJ, Yang F, Liu F, Zhao YG, Li DC. Precise estimation of soil organic carbon stocks in the northeast Tibetan plateau. Sci Rep. 2016;6:21842.
7. Yang S, Sheng D, Adamowski J, Gong Y, Zhang J, Cao J. Effect of land use change on soil carbon storage over the last 40 years in the Shi Yang River Basin, China. Land. 2018;7(1):11.
8. Beesley L. Carbon storage and fuxes in existing and newly created urban soils. J Environ Manag. 2012;104:158–65.
9. Wei ZQ, Wu SH, Zhou SL, Li JT, Zhao QG. Soil organic carbon transformation and related properties in urban soil under impervious surfaces. Pedosphere. 2014;24(1):56–64.
10. Golubiewski NE. Urbanisation increases grassland carbon pools: effects of landscaping in Colorado's front range. Ecol Appl. 2006;16(2):555–71.
11. Raciti SM, Hutryra LR, Finzi AC. Depleted soil carbon and nitrogen stocks under impervious surfaces. Environ Pollut. 2012;164:248–51.
12. Ait Ouhamchich K, Karaoui I, Arioua A, Kasmi A, Elhamdouni D, Elfiraoui E, Arioua Z, Nazi F, Nabih N. Climate change trend observations in Morocco: case study of Beni Mellal-Khenifra and Darâa-Tafilalt regions. J Geosci Environ Prot. 2018;6:34–50.
13. El Jazouli A, Barakat A, Khellouk R, Rais J, El Baghdadi M. Remote sensing and GIS techniques for prediction of land use land cover change effects on soil erosion in the high basin of the Oum Er Rbia River (Morocco). Remote Sens Appl Soc Environ. 2018;13:361–74.
14. Barakat A, Ouargaf Z, Khellouk R, El Jazouli A, Touhami F. Land use/land cover change and environmental impact assessment in Béni-Mellal district (Morocco) using remote sensing and GIS. Earth Syst Environ. 2019;3:1–13.
15. Baki Y, Boutoial K, Medaghri-Alaoui A. The impact of climate change on water inflow of the three largest dams in the Beni Mellal-Khenifra region. E3S Web Conf. 2021;314:03002.
16. Heuvelink GB, Angelini ME, Poggio L, Bai Z, Batjes NH, van den Bosch R, Sanderman J. Machine learning in space and time for modelling soil organic carbon change. Eur J Soil Sci. 2021;72(4):1607–23.
17. Odebiri O, Mutanga O, Odindi J, Naicker R. Modelling soil organic carbon stock distribution across different land-uses in South Africa: a remote sensing and deep learning approach. ISPRS J Photogramm Remote Sens. 2022;188:351–62.
18. Ahmed IS, Hassan FA, Sulieman MM, Keshavarzi A, Elmobarak AA, Yousif KM, Brevik EC. Using environmental covariates to predict soil organic carbon stocks in Vertisols of Sudan. Geoderma Reg. 2022;31: e00578.
19. Sanderman J, Baldock JA, Dangal SR, Ludwig S, Potter S, Rivard C, Savage K. Soil organic carbon fractions in the Great Plains of the United States: an application of mid-infrared spectroscopy. Biogeochemistry. 2021;156(1):97–114.
20. Ahmadi A, Emami M, Daccache A, He L. Soil properties prediction for precision agriculture using visible and near-infrared spectroscopy: a systematic review and meta-analysis. Agronomy. 2021;11(3):433.
21. Mousavi SR, Sarmadian F, Omid M, Bogaert P. Three-dimensional mapping of soil organic carbon using soil and environmental covariates in an arid and semiarid region of Iran. Measurement. 2022;201: 111706.
22. Tang X, Xia M, Pérez-Cruzado C, Guan F, Fan S. Spatial distribution of soil organic carbon stock in Moso bamboo forests in subtropical China. Sci Rep. 2017;7(1):42640.

23. Yao X, Yu K, Deng Y, Zeng Q, Lai Z, Liu J. Spatial distribution of soil organic carbon stocks in Masson pine (*Pinus massoniana*) forests in subtropical China. Catena. 2019;178:189–98.
24. Szatmári G, Pásztor L, Heuvelink GB. Estimating soil organic carbon stock change at multiple scales using machine learning and multivariate geostatistics. Geoderma. 2021;403:115356.
25. Wang S, Zhuang Q, Jia S, Jin X, Wang Q. Spatial variations of soil organic carbon stocks in a coastal hilly area of China. Geoderma. 2018;314:8–19. https://doi.org/10.1016/j.geoderma.2017.10.052.
26. Nguemezi C, Tematio P, Silatsa FB, Yemefack M. Spatial variation and temporal decline (1985–2017) of soil organic carbon stocks (SOCS) in relation to land use types in Tombel area, South-West Cameroon. Soil Tillage Res. 2021;213:105114.
27. Zeraatpisheh M, Garosi Y, Owliaie HR, Ayoubi S, Taghizadeh-Mehrjardi R, Scholten T, Xu M. Improving the spatial prediction of soil organic carbon using environmental covariates selection: a comparison of a group of environmental covariates. Catena. 2022;208:105723.
28. Odebiri O, Mutanga O, Odindi J, Naicker R, Slotow R, Mngadi M. Evaluation of projected soil organic carbon stocks under future climate and land cover changes in South Africa using a deep learning approach. J Environ Manag. 2023;330:117127.
29. Martin MP, Orton TG, Lacarce E, Meersmans J, Saby NPA, Paroissien JB, Arrouays D. Evaluation of modelling approaches for predicting the spatial distribution of soil organic carbon stocks at the national scale. Geoderma. 2014;223:97–107.
30. Bae J, Ryu Y. Land use and land cover changes explain spatial and temporal variations of the soil organic carbon stocks in a constructed urban park. Landsc Urban Plan. 2015;136(April):57–67.
31. Shifaw E, Sha J, Li X, Jiali S, Bao Z. Remote sensing and GIS-based analysis of urban dynamics and modelling of its drivers, the case of Pingtan, China. Environ Dev Sustain. 2018;22(3):2159–86.
32. Obeidat M, Awawdeh M, Lababneh A. Assessment of land use/land cover change and its environmental impacts using remote sensing and GIS techniques, Yarmouk River Basin, north Jordan. Arab J Geosci. 2019;12(22):685.
33. Fathizad H, Taghizadeh-Mehrjardi R, Hakimzadeh Ardakani MA, Zeraatpisheh M, Heung B, Scholten T. Spatiotemporal assessment of soil organic carbon change using machine-learning in arid regions. Agronomy. 2022;12(3):628.
34. Yan Y, Zhang C, Hu Y, Kuang W. Urban land-cover change and its impact on the ecosystem carbon storage in a Dryland city. Remote Sens. 2015;8(1):6.
35. Taghizadeh-Mehrjardi R, Neupane R, Sood K, Kumar S. Artificial bee colony feature selection algorithm combined with machine learning algorithms to predict vertical and lateral distribution of soil organic matter in South Dakota, USA. Carbon Manag. 2017;8(3):277–91.
36. Nurmiaty, Sumbangan B, Samsu A. GIS-based modelling of land use dynamics using cellular automata and Markov chain. J Environ Earth Sci. 2014;4(4):2224–3216.
37. Huong NTT, Phuong NTT. Land use/land cover change prediction in Dak Nong Province based on remote sensing and Markov Chain Model and Cellular Automata. J Vietnam Environ. 2018;9(3):132–40.
38. Baker WL. A review of models of landscape change. Landsc Ecol. 1989;2:111–33. https://doi.org/10.1007/BF00137155.
39. Muller MR, Middleton J. A Markov model of land-use change dynamics in the Niagara Region, Ontario, Canada. Landsc Ecol. 1994;9:151–7.
40. Sharjeel M, Zahir A, Mateeul H, Badar MG. Monitoring and predicting land use/landcover change using an integrated Markov chain & multilayer perceptron models: a case study of Sahiwal Tehsil. J GeoSpace Sci. 2016;1(2):43–59.
41. Hazhir K, Javad J, Jabbar K, Parisa A. Monitoring and prediction of land use/land cover changes using CA-Markov model: a case study of Ravansar County in Iran. Arab J Geosci. 2018;11(592):1–9.
42. Emadi M, Taghizadeh-Mehrjardi R, Cherati A, Danesh M, Mosavi A, Scholten T. Predicting and mapping of soil organic carbon using machine learning algorithms in Northern Iran. Remote Sens. 2020;12(14):2234.
43. Kılıc M, Gundoğan R, Gunal H, Cemek B. Accuracy assessment of Kriging, artificial neural network, and a hybrid approach integrating spatial and terrain data in estimating and mapping of soil organic carbon. PLoS One. 2022;17(5):e0268658.
44. Pouyat RV, Yesilonis ID, Nowak DJ. Carbon storage by urbain soils in the United States. J Environ Qual. 2006;35(4):1566–75.
45. Hutyra LR, Yoon B, Alberti M. Terrestrial carbon stocks across a gradient of urbanisation: a study of the Seattle, WA region. Glob Change Biol. 2011;17(2):783–97.
46. Kaye JP, McCulley RI, Burke IC. Carbon Fluxes, nitrogen cycling, and soil microbial communities in adjacent urban, native, and agricultural ecosystems. Glob Change Biol. 2005;11(4):575–87.
47. Mestdagh I, Sleutel S, Lootens P, Van Cleemput O, Carlier L. Soil organic carbon stocks in verges and urban areas of Flanders, Belgium. Grass Forage Sci. 2005;60(2):151–6.
48. Edmonds JL, O'Sullivan OS, Inger R, Potter J, McHugh N, Gaston KJ, Leake JR, Bond-Lamberty B. Urban tree effects on soil organic carbon. PLoS One. 2014;9(7): e101872.
49. Ministry of Agriculture, Fisheries, Rural, Development, Water and Forests.: Green Moroccan Plan. 2008.
50. Townshend JR, Masek JG, Huang C, Vermote EF, Gao F, Channan S, Sexton JO, Feng M, Narasimhan R, Kim D, Song K, Song D, Song XP, Noojipady P, Tan B, Hansen MC, Li M, Wolfe RE. Global characterisation and monitoring of forest cover using Landsat data: opportunities and challenges. Int J Digit Earth. 2012;5(5):373–97.
51. Gadal, S.; Oukhattar, M.; Keller, C. and Houmma, I.: Spatio-temporal modelling of relationship between organic carbon content and land use using deep learning approach and several co-variables: application to the soils of the Beni Mellal in Morocco. In: *Proceedings of the 9th International Conference on Geographical Information Systems Theory, Applications and Management*, 2023; pp. 15-26. https://doi.org/10.5220/0011723000003473.
52. Ennaji W, Barakat A, Karaoui I, El Baghdadi M, Arioua A. Remote sensing approach to assess salt-affected soils in the north-east part of Tadla plain, Morocco. Geol Ecol Landsc. 2018;2(1):22–8.
53. Aghzar N, Berdai H, Bellouti A, Soud B. Ground water nitrate pollution in Tadla (Morocco). J Water Sci Rev Sci Educ. 2002;15(2):459–92.
54. Hunter EL, Power CH. An assessment of two classification methods for mapping Thames Estuary intertidal habitats using CASI data. Int J Remote Sens. 2002;23(15):2989–3008.
55. Girouard G, Bannari A, El-Harti A, Desrochers A. Validated spectral angle mapper algorithm for geological mapping: comparative study between quickbird and Landsat-TM, geo-imagery bridging continents Istanbul, Turkey. Environ Sci Math Geol. 2004;12(23):599–604.
56. Kruse FA, Lefkoff AB, Boardman JW, Heidebrecht KB, Shapiro PJ, Goetz AFH. The spectral image processing system (SIPS)-interactive visualisation and analysis of imaging spectrometer data. Remote Sens Environ. 1993;44(2–3):145–63.
57. Adams WA. The effect of organic matter on the bulk and true densities of some uncultivated podzolic soils. Eur J Soil Sci. 1973;24:10–7.
58. Cresswell HP, Hamilton GJ, et al. Bulk density and pore space relations. In: McKenzie NJ, et al., editors. Soil physical

measurement and interpretation for land evaluation. Australian Soil and Land Survey Handbook. CSIRO; 2002. p. 35–58.
59. What is soil organic carbon? Agriculture and Food. 2022. https://www.agric.wa.gov.au/measuring-and-assessing-soils/what-soil-organic-carbon.
60. Total Organic Carbon, Fact Sheets. soilquality.org.au. https://www.soilquality.org.au/factsheets/organic-carbon.
61. Schneider F, Poeplau C, Don A. Predicting ecosystem responses by data-driven reciprocal modelling. Glob Change Biol. 2021;27(21):5670–9. https://doi.org/10.1111/gcb.15817.
62. Lugato E, Panagos P, Bampa F, Jones A, Montanarella L. A new baseline of organic carbon stock in European agricultural soils using a modelling approach. Glob Change Biol. 2014;20(1):313–26.
63. FAO. Measuring and modelling soil carbon stocks and stock changes in livestock production systems: Guidelines for assessment (Version 1). *Livestock Environmental Assessment and Performance (LEAP) Partnership. Rome, FAO*. 170 pp. Licence: CC BY-NC-SA 3.0 IGO. 2019.
64. Pacini L, Arbelet P, Chen S, Bacq-Labreuil A, Calvaruso C, Schneider F, Arrouays D, Saby NPA, Cécillon L, Barré P. A new approach to estimate soil organic carbon content targets in European croplands topsoils. Sci Total Environ. 2023;900:165811. https://doi.org/10.1016/j.scitotenv.2023.165811.
65. Garcia-Gaines, A., Frankenstein, S.: USCS and the USDA soil classification system. In: *US army corps of engineers*. 2015; pp. 46
66. Gidey E, Dikinya O, Sebego R. Cellular automata and Markov Chain (CA-Markov) model-based predictions of future land use and land cover scenarios (2015–2033) in Raya, northern Ethiopia. Model Earth Syst Environ. 2017;3:1245–62.
67. Gadal, S., Oukhattar, M., Otobo, S.O.: Multitemporal recognition of built-up area and land cover changes using machine learning approach in the Metropolis of Aix-Marseille-Provence in France. In: *2023 Joint Urban Remote Sensing Event (JURSE)*, Heraklion, Greece. 2023; pp. 1-4. https://doi.org/10.1109/JURSE57346.2023.10144184.
68. Rwanga S, Ndambuki J. Accuracy assessment of land use/land cover classification using remote sensing and GIS. Int J Geosci. 2017;8:611–22. https://doi.org/10.4236/ijg.2017.84033.
69. Emamgholizadeh S, Esmaeilbeiki F, Babak M, Zarehaghi D, Maroufpoor E, Rezaei H. Estimation of the organic carbon content by the pattern recognition method. Commun Soil Sci Plant Anal. 2018;49(17):2143–54.
70. Muchena R. Estimating soil carbon stocks in a dry Miombo ecosystem using remote sensing. For Res Open Access. 2017. https://doi.org/10.4172/2168-9776.1000198.
71. Zomer RJ, Neufeldt H, Xu J, Ahrends A, Bossio D, Trabucco A, Wang M. Global tree cover and biomass carbon on agricultural land: the contribution of agroforestry to global and national carbon budgets. Sci Rep. 2016;6(1):29987.
72. Bogunovic I, Viduka A, Magdic I, Telak LJ, Francos M, Pereira P. Agricultural and forestland-use impact on soil properties in Zagreb periurban area (Croatia). Agronomy. 2020;10(9):1331.
73. Laganière J, Déni AA, David P. Carbon accumulation in agricultural soils after afforestation: a meta-analysis. Glob Change Biol. 2010;16(1):439–53.
74. Ghimire P, Bhatta B, Pokhrel B, Kafle G, Paudel P. Soil organic carbon stocks under different land uses in Chure region of Makawanpur district, Nepal. SAARC J Agric. 2019;16:13–23. https://doi.org/10.3329/sja.v16i2.40255.
75. Reicosky DC. Tillage-induced CO_2 emissions and carbon sequestration: effect of secondary tillage and compaction. Conserv Agric Environ Farmers Exp Innov Socioecon Policy. 2003. https://doi.org/10.1007/978-94-017-1143-2_35.
76. Haddaway NR, Hedlund K, Jackson LE, et al. How does tillage intensity affect soil organic carbon? A systematic review. Environ Evid. 2017;6:30. https://doi.org/10.1186/s13750-017-0108-9.
77. Ramesh T, Bolan NS, Kirkham MB, Wijesekara H, Kanchikerimath M, Rao CS, Freeman OW II. Soil organic carbon dynamics: impact of land use changes and management practices: A review. Adv Agron. 2019;156:1–107.
78. Xiong X, Grunwald S, Myers DB, Ross CW, Harris WG, Comerford NB. Interaction effects of climate and land use/land cover change on soil organic carbon sequestration. Sci Total Environ. 2014;493:974–82.
79. Buraka T, Elias E, Lelago A. Soil organic carbon and its' stock potential in different land-use types along slope position in Coka watershed, Southern Ethiopia. Heliyon. 2022;8(8):e10261.

Authors and Affiliations

Sébastien Gadal[1] · Mounir Oukhattar[1,2] · Catherine Keller[2] · Ismaguil Hanadé Houmma[1,3]

✉ Mounir Oukhattar
mounir.oukhattar@etu.univ-amu.fr

Sébastien Gadal
sebastien.gadal@univ-amu.fr

Catherine Keller
keller@cerege.fr

Ismaguil Hanadé Houmma
ismaguil.hanade-houmma@etu.univ-amu.fr

[1] Aix-Marseille University, CNRS, ESPACE UMR 7300, University, Nice Sophia Antipolis, Avignon University, 13545 Aix-en-Provence, France

[2] Aix-Marseille University, CNRS, IRD, INRAE, CEREGE, Technopole de l'Environnement Arbois-Méditerranée, BP80, 13545 Aix-en-Provence, France

[3] Department of Geodesy and Topography, Geomatics Science and Engineering, Hassan II Institute of Agronomy and Veterinary, Rabat, Morocco